Powertech

Powertech Labs Inc. 12388 – 88th Avenue
Surrey, British Columbia
Canada V3W 7R7

Tel: (604) 590-7500
Fax: (604) 590-5347
www.powertechlabs.com

Final Report (Public)

Small-Signal Stability Study for ERCOT

Powertech Project: PL-00323
Report No.: PL-00323-5

Prepared by

Powertech Labs Inc. (PLI)

Prepared For

Electric Reliability Council Of Texas (ERCOT), Inc.
7620 Metro Center Dr.
Austin, Texas 78744-1654

August 2014

Prepared by: _____
Saeed Arabi, Ph.D.
Principal Engineer, Power System Studies
Phone: (604) 590-7459
Email: saeed.arabi@powertechlabs.com

Approved by: _____
Zhihong Feng, Ph.D.
Manager, Power System Studies
Phone: (604) 590-7477
Email: zhihong.feng@powertechlabs.com

Acknowledgements

The Powertech project team appreciates the assistance of the following ERCOT personnel:

Mr. Jose Conto
Dr. Shun-Hsien (Fred) Huang

The contributions of the following Powertech personnel to this project are also acknowledged:

Mr. Pooya Taheri
Dr. Lei Wang
Dr. Fred Howell
Dr. Xi Lin

Executive Summary

A comprehensive small-signal stability analysis was performed for the ERCOT interconnected system. The study was focused on the following three aspects:

- To perform a comprehensive examination of the small-signal stability situation of the ERCOT system, particularly the sensitivities of the critical system modes with respect to different system conditions, transfer patterns, and various contingencies;
- To provide recommendations for tuning the existing Power System Stabilizers (PSS) and adding new PSS in the ERCOT system to accomplish optimal performance for identified critical modes without adverse effects;
- To identify the best Phasor Measurement Unit (PMU) locations for oscillation monitoring.

The small-signal stability analysis was conducted for the following system representations:

- Two system conditions, i.e., peak load and light load with high wind generation;
- Five transfer patterns in each condition to create the worst-case scenarios for damping situations;
- Single, double, and multiple extreme contingencies for all transfer patterns and loading conditions.

Two complementary approaches were used in this study to ensure robustness of the process:

- Modal analysis of linearized system based on eigenvalue techniques;
- Non-linear time-domain simulations with both small and large disturbances.

Both local and inter-area modes of oscillation were analyzed. Critical modes along with their modal characteristics were identified. In particular, a two-plant mode was found to be prone to negative damping in certain extreme contingency situations, as well as an inter-area mode with potentially poor damping under certain extreme conditions. Based on the findings, seven new PSS were proposed. Tuned settings for optimal performance of 141 existing PSS were also produced, 39 of which were recommended to be modified in the field (the remaining 102 were not significantly far from optimum). Moreover, voltage magnitude mode shapes were utilized to identify the best locations for small-signal monitoring using PMUs.

The substations for installation of PMUs to monitor inter-area oscillations may be selected from the ranked list below:

#	Bus # [Name]	#	Bus # [Name]	#	Bus # [Name]
1	8905 [NEDIN7C 345.]	13	3105 [ELKTON_5345.]	25	45500 [T_H_W___345.]
2	5915 [SO_TEX__345.]	14	45971 [KUYDAL74345.]	26	46100 [N_BELT__345.]
3	3100 [MARTINLK345.]	15	3103 [SHAMBRGR345.]	27	40700 [GRNBYU__345.]

4	40600 [ROANS___345.]	16	3119 [NACOGDSE345.]	28	3130 [FOREGROV345.]
5	44645 [SNGLTN_3345.]	17	46290 [RTHWOD__345.]	29	3124 [TRINDAD2345.]
6	967 [GIBN_CRE345.]	18	3117 [LUFKNSS_345.]	30	3123 [TRINDAD1345.]
7	45972 [KUYDAL75345.]	19	80307 [DELSOL7B345.	31	80355 [DELSOL7A345.
8	42500 [DOW_____345.]	20	8902 [RIOHONDO345.]	32	43035 [OASIS___345.]
9	46500 [TOMBAL__345.]	21	44900 [ZENITH__345.]	33	5966 [LALTA345345.
10	3102 [TYLERGND345.]	22	8164 [COLETO7A345.]	34	43030 [MEADOW__345.]
11	3116 [MTENTRPR345.]	23	44200 [HILLJE__345.]		
12	3109 [STRYKER_345.]	24	40900 [KING____345.]		

ERCOT may choose from the above list considering the suitability of the associated substations for PMU installation (or PMU availability at present). In particular, the first four substations provide high observability for all six modes, although inclusion of more locations may be considered to increase the reliability of the monitoring system. Once a location is chosen, however, any nearby bus is redundant and may be skipped.

The eigenvalue analysis, the PSS tuning procedure, and the PMU placement for oscillation monitoring, as well as their time-domain verifications, performed in this study are described in detail in this report. All findings and conclusions are documented. The pertinent data files used in the study are also made available to ERCOT.

The study reveals that small-signal stability is indeed a security concern for the ERCOT system, where PSS play an essential role in providing sufficient damping to the low-frequency oscillatory modes. It is therefore recommended that similar studies be performed regularly to ensure the small-signal security of the system. The following may serve as guiding indicators for initiating future studies of this nature, especially if they occur in the areas that are already identified to be prone to damping issues:

- Addition/retirement of sizable generation (and generator controls);
- Significant load increases, both static (non-rotating) and dynamic (induction motors);
- Major expansions/interconnections of the transmission system;
- Indication of a poorly-damped oscillation in the system by monitoring devices.

Furthermore, the following should be emphasized in future studies of similar nature:

- Completeness of the dynamic data as much as possible;
- Accuracy of the data, particularly for the generator excitation system models;
- System operating conditions, including the level of wind and other renewable generations.

Table of Contents

Executive Summary 3
1. Introduction 10
1.1 Background 10
1.2 Objectives 10
2. Scope and Approach 11
2.1 Project Scope 11
2.2 Study Approach 11
2.3 Analysis Tools 12
2.4 Robustness of the Study Process 13
2.5 Deliverables 13
3. Model Assembly and Data Checking 14
3.1 Base Model Descriptions 14
3.2 Base Model Data Modifications 14
3.3 Load Models 15
3.4 Contingencies 15
3.5 Transfer Paths 16
3.6 Simulation Programs Setup Options 16
4. Creation of Transfer Scenarios 18
4.1 Peak Load Transfer Scenarios 18
4.2 Light Load Transfer Scenarios 18
4.3 Voltage Stability Comments 19
5. Eigenvalue Analysis 20
5.1 Peak Load Inter-area Mode Analysis 20
5.2 Light Load Inter-area Mode Analysis 21
5.3 Local Mode Analysis 21
5.4 Best PMU Locations for Small-signal Stability Monitoring 23
5.5 Load Model Sensitivity 28
5.6 Wind Generation Dynamics Impact 29
5.7 Time-domain Verifications 30
6. Tuning of Power System Stabilizers 34
6.1 Tuning Procedure 34
6.1.1 Washout Time Constant 34
6.1.2 Phase Compensation 36
6.1.3 Gain Setting 37
6.2 Tuning of the New PSS 38
6.3 Tuning of the Existing PSS 40
6.4 Performance of the New PSS 42
6.5 Performance of the Existing PSS 47
6.6 Assessment of a Recent Event in Houston 52
6.7 Comparison with the Previous Study of the Same Nature 55
7. Conclusions 56
7.1 Summary of the Findings 56

7.2 Recommendations for Future Studies....58
8. References....59
9. Appendix A: Weather and Service Areas and Zones of ERCOT....60
10. Appendix B: Contents of the Transferred Files....62
10.1 VSAT Files....62
10.2 SSAT Files....62
10.3 TSAT Files....62

List of Tables

Table 3-1: Power Flow Summary of Base Cases....14
Table 3-2: Applied Contingencies in Both Voltage Stability and Eigenvalue Analyses. 16
Table 3-3: Applied Transfer Paths. 16
Table 4-1: FY2018 Voltage Stability Limits before Applying Margin. 18
Table 4-2: HWLL2016 Voltage Stability Limits before Applying Margin. 18
Table 5-1: FY2018 Lowest-damped Inter-area Modes. 21
Table 5-2: HWLL2016 Lowest-damped Inter-area Modes. 21
Table 5-3: Local (Two-plant) Mode with Damping Issue Using Full Model. 22
Table 5-4: Local (Two-plant) Mode with Damping Issue Using Simplified Model. 22
Table 5-5: Modes of Interest for Monitoring by PMUs. 24
Table 5-6: Voltage Magnitude Mode Shape Entries for Mode of Interest #1. 24
Table 5-7: Voltage Magnitude Mode Shape Entries for Mode of Interest #2. 25
Table 5-8: Voltage Magnitude Mode Shape Entries for Mode of Interest #3. 25
Table 5-9: Voltage Magnitude Mode Shape Entries for Mode of Interest #4. 26
Table 5-10: Voltage Magnitude Mode Shape Entries for Mode of Interest #5. 26
Table 5-11: Voltage Magnitude Mode Shape Entries for Mode of Interest #6. 27
Table 5-12: Best Monitoring Buses for All Modes of Interest (Ranked). 27
Table 5-13: Sensitivity of Critical Modes to Load Models. 29
Table 5-14: Wind Generation Impact on Critical Modes. 29
Table 5-15: Mode Comparisons of the Existing System. 30
Table 5-16: Suggested Buses for Oscillation Monitoring Comparisons. 31
Table 6-1: Suggested PSS Parameter Corrections. 40
Table 6-2: Suggested PSS Phase Tunings. 41
Table 6-3: Suggested PSS Gain Tunings. 42
Table 6-4: Mode Comparisons for New PSS Performance. 42

List of Figures

Figure 2-1: Study Procedure Chart. 12
Figure 5-1: Small-disturbance Time-domain Responses for the Critical Inter-area Mode. 32
Figure 5-2: Small-disturbance Time-domain Responses for the Critical Local (Two-plant) Mode. ...32
Figure 5-3: FY2018 Large-disturbance Simulation Results for Oscillation Monitoring. 33
Figure 5-4: HWLL2016 Large-disturbance Simulation Results for Oscillation Monitoring. 33
Figure 6-1: Frequency Characteristics of Washout Functions....35
Figure 6-2: K_{S2}/T_7 Block of the PSS2A and PSS2B Models with Speed and Power Inputs....35
Figure 6-3: Example of a Lead Function Providing Maximum 60 Degrees at 3 Hz. 36
Figure 6-4: Example of PSS Phase Compensation Design. 37
Figure 6-5: Root Locus Example. 37
Figure 6-6: PSS Phase Compensation for a Unit Corresponding to the Critical Inter-area Mode. 38
Figure 6-7: PSS Phase Compensation for a Unit of Plant 1 Corresponding to the Critical Local Mode. 39
Figure 6-8: PSS Phase Compensation for a Unit of Plant 2 Corresponding to the Critical Local Mode. 39
Figure 6-9: New PSS Performance for the Critical Inter-area Mode. 44
Figure 6-10: New PSS Performance for the Critical Local (Two-plant) Mode....44
Figure 6-11: New PSS Output for the Large Disturbance #1. 45
Figure 6-12: New PSS Outputs for the Large Disturbance #2. 45
Figure 6-13: Active Power Comparison for the Large Disturbance #1. 46
Figure 6-14: Active Power Comparison for the Large Disturbance #2. 46
Figure 6-15: Existing PSS Outputs for the Large Disturbance #1 – FY2018 Base Case before Tuning. 48
Figure 6-16: Existing PSS Outputs for the Large Disturbance #1 – FY2018 Base Case after Tuning. 48
Figure 6-17: Existing PSS Outputs for the Large Disturbance #2 – FY2018 Base Case before Tuning. 49
Figure 6-18: Existing PSS Outputs for the Large Disturbance #2 – FY2018 Base Case after Tuning. 49
Figure 6-19: Existing PSS Outputs for the Large Disturbance #1 – HWLL2016 Base Case before Tuning. 50
Figure 6-20: Existing PSS Outputs for the Large Disturbance #1 – HWLL2016 Base Case after Tuning. 50
Figure 6-21: Existing PSS Outputs for the Large Disturbance #2 – HWLL2016 Base Case before Tuning. 51
Figure 6-22: Existing PSS Outputs for the Large Disturbance #2 – HWLL2016 Base Case after Tuning. 51
Figure 6-23: Active Power Responses of Unit 4 of Plant X before and after Sign Inversion in Its Exciter – FY2018 Base Case. 54
Figure 6-24: Field Voltage Responses of Unit 4 of Plant X before and after Sign Inversion in Its Exciter – FY2018 Base Case. 54
Figure 9-1: Weather Zones and Texas Counties. 60
Figure 9-2: Service Areas/Zones of ERCOT. 61

1. Introduction

1.1 Background

Small-signal stability is one form of the angle stability commonly observed in power systems. It refers to the ability of a power system to withstand small disturbances in a system. Small-signal stability problems usually appear as poorly/negatively damped oscillations in the system, which often cause security violations. They might even lead to system-wide blackouts such as the event that occurred in WECC on August 10, 1996 [1].

Unlike traditional transient stability analysis in which large disturbances (such as short-circuit faults and the subsequent line trips) are applied, in small-signal stability analysis disturbances are assumed to be sufficiently small so that the dynamic characteristics of the system can be linearized, thus enabling the use of many powerful analysis tools. One such tool is *modal analysis* based on eigenvalue techniques. This method can identify critical modes of oscillations in the system along with their characteristics. The eigenvalue analysis, used in combination with non-linear time-domain simulations, can effectively give solutions to small-signal stability problems, including analysis of local and inter-area oscillations, as well as the application of Power System Stabilizers (PSS). References [2] and [3] contain useful background material on the theory and analysis of the small-signal stability of power systems.

This project examined the ERCOT interconnected system from the small-signal stability perspective. Critical system modes were identified and traced for various system loadings, transfer patterns, and contingencies. The results give good indications of the small-signal stability behavior of the system, i.e., sensitivities of the critical system modes with respect to various operating conditions. Guided by these results, proposed new and existing PSS settings were developed to provide optimal damping for the critical modes without adverse effects. Note that a similar study was performed on ERCOT system in 2001-2002 [4].

1.2 Objectives

The objectives of this study are the following:

- To perform a comprehensive examination of the small-signal stability of the ERCOT interconnected system, particularly the sensitivities of the critical system modes with respect to different system conditions, transfer patterns, and contingencies;
- To provide recommendations for tuning the existing PSS and adding new PSS in the ERCOT system to accomplish optimal performance for identified critical modes without adverse effects;
- To identify the best Phasor Measurement Unit (PMU) locations for low frequency oscillation monitoring.

2. Scope and Approach

2.1 Project Scope

This study used the most current data available from ERCOT with consideration of the near-term proposed generation, load, and transmission facility additions. The study included the following:

- A reasonability check of system dynamic data;
- Creation of five transfer scenarios from each of the two base power flows provided by ERCOT using voltage stability analysis with the pre-contingency and all NERC (North-American Electric Reliability Corporation) category B, C, and D contingencies provided by ERCOT, as well as scanning of all 345 kV single branches;
- Eigenvalue analysis for the created scenarios with the pre-contingency and contingencies similar to those above, to assess the small-signal performance of the ERCOT system;
- Determination of PSS settings to provide optimal performance in the ERCOT system, including the existing and newly proposed PSS;
- Time-domain verification of the effectiveness of the PSS settings for various system conditions and contingencies;
- Identification of the best PMU locations for oscillation monitoring;
- Discussions around load sensitivity, wind generation dynamics impact, 2012 Houston oscillations event, and how the results compare to the 2001-2002 study of similar nature.

2.2 Study Approach

As described earlier, three main factors affecting system conditions were studied in this project, namely, loading conditions, transfer patterns, and contingencies. It is obvious that every possible combination of these factors can easily lead to a huge number of scenarios, which will be not only impractical but also unnecessary to study in detail. In order to maintain a manageable number of scenarios to be studied, while still providing sufficient study breadth to fulfill the project scope, the number of loading conditions and transfer patterns were limited to two and five, respectively. On the other hand, sweeping numbers of contingencies of various types were applied. Moreover, the following study procedure was used:

- A scenario was defined as a combination of a loading condition and a transfer pattern. As a result, 12 scenarios were set up (including base scenarios with no transfer);
- All inter-area modes in the frequency range of 0.2-1.0 Hz with damping ratio[1] less than 10% were computed for the defined scenarios in pre-contingency and in all contingency situations;

[1] An oscillatory mode corresponds to a pair of eigenvalues, $\alpha \pm j\omega$, of the linearized system. The mode frequency in Hz is $f = \omega / (2\pi)$, and its damping ratio in percentage (or simply damping) is defined as $\xi = -100\,\alpha / (\alpha^2 + \omega^2)^{1/2}$.

- Local modes were generally analyzed using Single-Machine Infinite-Bus (SMIB) scans, and then eigenvalue range was applied for further investigations of critical situations;
- New PSS were proposed and tuned for the critical modes, while the existing PSS were tuned for optimal damping without adverse effects;
- Best PMU locations for oscillation monitoring were identified using voltage magnitude mode shapes of the selected modes having the lowest damping ratios;
- Time-domain simulations were performed to selectively verify eigenvalue findings and important characteristics related to both small and large disturbances.

The procedure for the whole study is illustrated in Figure 2-1.

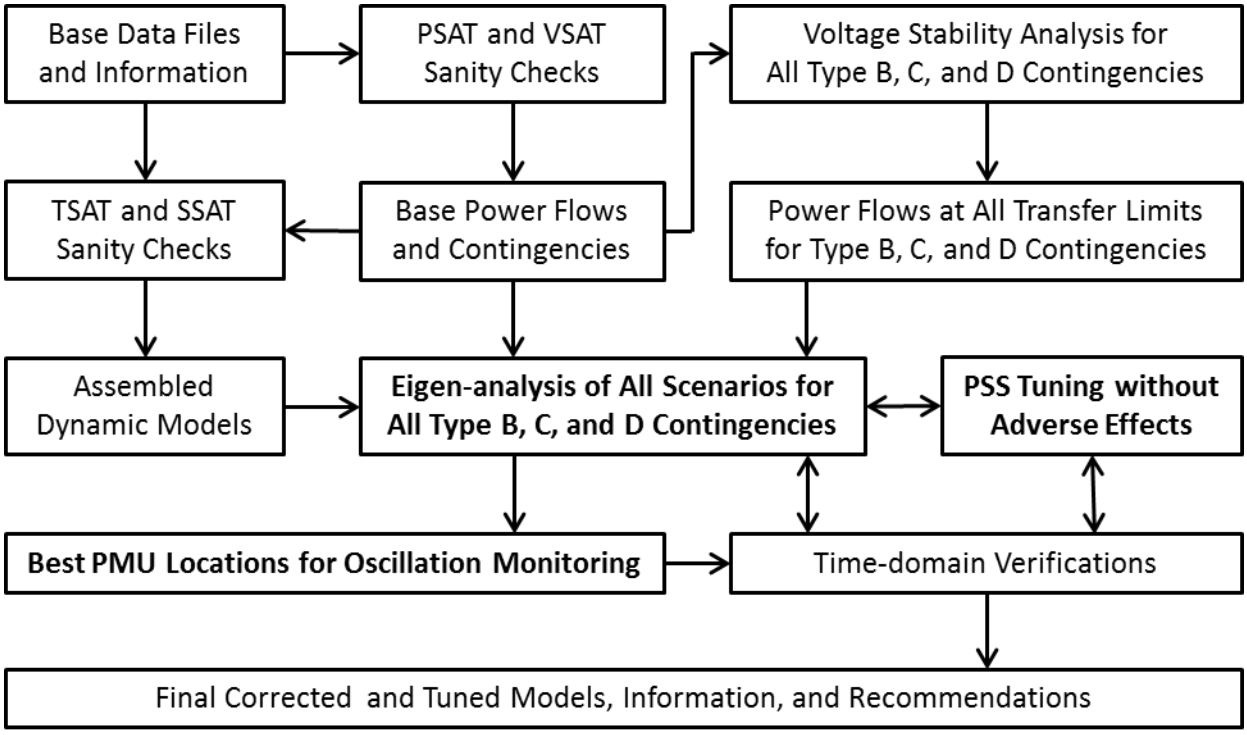

Figure 2-1: Study Procedure Chart.

2.3 Analysis Tools

Powertech's DSATools™ was used in this study. This package includes the following main programs:

- Power-flow and Short-circuit Analysis Tool (PSAT): This program was used to set up all relevant power flows.

- Voltage Security Assessment Tool (VSAT): This program was used to dispatch the base models provided by ERCOT to obtain transfer scenarios.
- Small-signal Stability Analysis Tool (SSAT): This program was used to perform eigenvalue analysis of all scenarios, as well as making the first assessment of the effectiveness of the newly proposed and tuned existing PSS.
- Transient Security Assessment Tool (TSAT): This program was used to verify eigenvalue analysis results with time-domain simulations, and to determine optimal PSS gain and limit settings for the newly proposed PSS.

2.4 Robustness of the Study Process

The study procedure and tools selected in this project are a robust combination for small signal stability analysis. In particular, the following points may be noted:

- *Model assembly:* There are many unique sanity checking capabilities in all programs of DSATools™ which are extensively applied to set up the appropriate models.
- *Creation of the worst-case power flow scenarios:* VSAT powerful capabilities are used to create the intended transfers at the highest possible levels by applying comprehensive lists of all types of contingencies, provided and scanned.
- *Modal analysis:* As damping is mostly a linear issue, the utilization of SSAT eigenvalue-analysis capabilities renders a vast amount of decoupled information about not only the frequency and damping of all types of critical low-frequency oscillations, but also about the signature of the modes, best locations for application of damping controls, optimization of PSS tunings, best locations for oscillation monitoring, etc.
- *Time-domain verifications:* The above analyses and screenings greatly reduce the need for otherwise completely impractical transient stability simulations of comprehensive contingencies and scenarios; they direct the non-linear simulation requirements to a handful of disturbance applications under the worst conditions. The obtained verifications provide for a high level of confidence in the right discovery of critical modes and the overall conclusions.

2.5 Deliverables

The deliverables of this project include the following:

- This final report;
- Data files to run VSAT, SSAT, and TSAT relevant cases (see Appendix B);
- A presentation of the study findings and conclusions to ERCOT;
- A small-signal stability training course for ERCOT.

3. Model Assembly and Data Checking

3.1 Base Model Descriptions

ERCOT provided two base power flow models in PSS/E RAWD format representing the following loading conditions:

- Year 2018 peak load (FY2018);
- Year 2016 light load with high wind generation (HWLL2016).

The power flow summaries for these models are tabulated in Table 3-1. ERCOT also provided the matching dynamic data files in PSS/E format. The base power flow models were modified to include the ERCOT Weather Zones information as area data while the Texas County information was included as zone data. The Weather Zones are intended to identify the likely transfer patterns. The maps showing the two sets are included in Appendix A.

Table 3-1: Power Flow Summary of Base Cases.

Base Case	Area		Generation		Load	
	Name	#	MW	MVAr	MW	MVAr
FY2018 (Peak Load)	COAST	101	21224	4770	23847	5311
	EAST	102	12554	1506	2849	723
	NORTH	103	4499	501	1750	462
	NORTH_CENTRA (DFW Counties)	104 (In 104)	18099 (8039)	2065 (1319)	26551 (21831)	7502 (6237)
	SOUTH_CENTRA	105	13242	3332	13845	4126
	SOUTHERN	106	6837	951	5444	1805
	FAR_WEST	107	3101	372	3153	951
	WEST	108	2044	-360	2283	675
		Total	**81599**	**13136**	**79721**	**21553**
HWLL2016 (High Wind, Light Load)	COAST	101	9545	1999	13689	2477
	EAST	102	5752	-238	1177	337
	NORTH	103	1721	-115	727	127
	NORTH_CENTRA (DFW Counties)	104	6762 (1304)	366 (298)	9667 (7985)	1976 (1659)
	SOUTH_CENTRA	105	3993	254	4934	1242
	SOUTHERN	106	3276	376	3338	826
	FAR_WEST	107	2106	-373	1578	484
	WEST	108	4096	-31	1156	296
		Total	**37250**	**2237**	**36266**	**7765**

3.2 Base Model Data Modifications

Through the conversion from RAW data file to PSAT, data corrections were manually implemented.

Through the case setup for SSAT and TSAT, a number of dynamic data corrections and special model conversions were implemented in consultation with ERCOT (communicated to resource entities and suggested for implementation in the model without delaying the study progress).

Exciter step response (5%), governor step response (1%), and no-disturbance (10-s) response facilities of TSAT were utilized in the above process, as well as the ring down 30s-disturbance test. Exciter and governor step responses indicated unstable oscillations for Mach1 and Mach2 units. After implementing the modifications described above, these issues became satisfactory, and a flat no-disturbance response was obtained. The ring down test also produced responses similar to the original case in PSS/E.

Single-Machine-Infinite-Bus (SMIB) eigenvalue scan of all synchronous generators was also performed by SSAT for sanity checking of the data, which did not show any damping issue after the final setups. Further sanity checking was conducted for all wind generators and other devices revealing no data issues.

3.3 Load Models

In both SSAT and TSAT dynamic simulations static load models were applied and their coefficients "KI%, KZ%, KP%" were set to "50%, 50%, 0%" for active power and "0%, 50%, 50%" for reactive power components, respectively. Load model sensitivities were also performed for SSAT by making these coefficients stiffer, as well as converting part of the models to dynamic (induction motors) components, as specified later. Note that in VSAT all loads are modeled as constant power for both active and reactive power components.

3.4 Contingencies

Four sets of contingencies were applied in VSAT and SSAT cases:

- All 345 kV single-branch outages, i.e., N-1, scanned by Powertech;
- All NERC category B contingencies, i.e., N-1, provided by ERCOT;
- All NERC category C contingencies, i.e., N-2 (or N-1-1), provided by ERCOT;
- All NERC category D contingencies, i.e., N-x, provided by ERCOT.

The numbers of the above contingencies in each base case are presented in Table 3-2. Note that only a limited number of small and large disturbances were selected for application in TSAT, which are described later in time-domain verification simulations. Furthermore, based on the single-contingency results some combinations of generator and branch outages were applied in SSAT (i.e., G-1-1), which are discussed later along with the eigenvalue analysis.

Table 3-2: Applied Contingencies in Both Voltage Stability and Eigenvalue Analyses.

Base Case	# of 345 kV Scanned Contingencies (N-1)	# of Valid Specified Contingencies			Total #
		Type B (N-1)	Type C (N-2)	Type D (N-x)	
FY2018	817	1219	3556	477	6069
HWLL2016	796	1220	3539	473	6028

3.5 Transfer Paths

Five transfer paths were set up as described in Table 3-3. ERCOT specified the generation-load dispatches for achieving these transfers, which were different under the two loading conditions; they are defined in the next section.

Table 3-3: Applied Transfer Paths.

Import Name	Sink Areas or Zones	Participating Source Areas
Houston	Coast (101)	Far West (107), West (108), North (103), North Central (104), East (102)
Rio Grande Valley (RGV)	Southern (106)	Far West (107), West (108), North (103), North Central (104), East (102)
Dallas Fort Worth (DFW)	FDW Counties: Collin (43), Dallas (57), Denton (62), Ellis (71), Hunt (116), Kaufman (126), Johnson (129), Rockwall (199), Tarrant (220)	Far West (107, West (108), North (103), Southern (106), East (102)
West	West (108)	Far West (107), Southern (106, North (103), North Central (104), East (102)
Far West	Far West (107)	West (108), Southern (106), North (103), North Central (104), East (102)

3.6 Simulation Programs Setup Options

All VSAT cases were set up with the following options:

- Switched-shunt controls turned on in both pre- and post-contingency situations (to reach the maximum voltage stability limits);
- Under-Load Tap-Changer (ULTC) controls turned on in both pre- and post-contingency situations (to reach the maximum voltage stability limits);
- Phase-shifter controls turned off after base-case solutions, which ensure correct solution with Variable Frequency Transformer (VFT) represented by a phase-shifter model (i.e., for correct re-solving of the post-contingency power flows);
- Governor response, assuming all machines to have the same droop, turned on for contingency solutions, which ensures that any load-generation imbalance (due to variations in thermal losses, load/generation isolations, etc.) is distributed on all machines rather than just applied to the swing generator.

All SSAT cases were set up with the following options:

- "Torque" solution for generator swing equation, which generally produces slightly worse results than the "power" solution option (to consider the worst-case situation); this is recommended as it provides a worst-case condition and is also consistent with PSS/E modeling.
- "Full" generator saturation model, which produced essentially the same results as those of "incremental" option; the actual effect of non-linear saturation is generally expected to be within these two options but usually closer to the former;
- Respecting power-flow load models, which ensures correct allocation of the load model coefficients (i.e., "KI%, KZ%, KP%" for both P and Q);
- The unit governors of a plant that does not respond to frequency events were disabled.

All TSAT cases were also setup with options consistent with those of SSAT cases. Furthermore, a time step of 0.004 second was used in all TSAT cases.

4. Creation of Transfer Scenarios

VSAT was run with the five import transfers on both base power flows for all NERC category B, C, and D specified contingencies, as well as for all 345 kV single-branch scanned contingencies. The results are presented below. The power flows at the transfer limits are saved for the dynamic analysis.

4.1 Peak Load Transfer Scenarios

In FY2018 case source generation was scaled up versus scaling up the sink load in steps of 500 MW with 50 MW cut-off (refined) steps. The load increase, rather than generation decrease, of the sink region ensures highest flows through the associated transmission network. The results are summarized in Table 4-1. Note that the sink initial MW values are the corresponding non-negative scalable loads. Note that negative loads are generations without a specific model.

Table 4-1: FY2018 Voltage Stability Limits before Applying Margin.

Import Name	Initial MW	Possible MW Transfer Increase			First Limiting Contingency		
	Sink	Type B	Type C	Type D	Type B	Type C	Type D
Houston	22664	3500	1375	300	Scan_44645-46500-74	DB_ID_5545	DB_ID_9190
RGV	7084	1250	675	1725*	DB_ID_3537	DB_ID_884	DB_ID_17991
DFW	21768	2600	2425	4350*	DB_ID_15045	DB_ID_884	Pre-contingency
West	2294	1300	375	1925*	DB_ID_13284	DB_ID_3020	DB_ID_11187
Far West	2993	875	250	600	DB_ID_16053	DB_ID_15616	DB_ID_15961

* Is Lowered to Limit Found for Type B

4.2 Light Load Transfer Scenarios

In HWLL2016 case source generation was scaled up versus reducing sink Natural Gas (NG) generation in steps of 500 MW with 50 MW cut-off (refined) steps. West and Far West sinks were already at their minimum, and RGV and DFW sinks reached their minimum generations before reaching their Voltage Stability (VS) limits. Thus, a second transfer was applied to each of these four cases by scaling up the sink loads until VS limits were reached. The reported MW increases, presented in Table 4-2, are then the sum of these two steps. Note that the sink initial MW values are the corresponding non-negative scalable loads (consistent with the 2nd transfer and peak load reporting).

Table 4-2: HWLL2016 Voltage Stability Limits before Applying Margin.

Import Name	Initial MW	Possible MW Transfer Increase			First Limiting Contingency		
	Sink	Type B	Type C	Type D	Type B	Type C	Type D
Houston	10863	2175	250	1100	DB_ID_3416	DB_ID_2412	DB_ID_7803
RGV	3338	1633	1083	1758*	DB_ID_3772	DB_ID_697	DB_ID_9296
DFW	7972	4051	3726	5476*	DB_ID_3772	DB_ID_2616	DB_ID_6723
West	1174	1875	1550	2500*	DB_ID_11101	DB_ID_653	DB_ID_18739
Far West	1441	925	550	800	DB_ID_14077	DB_ID_15616	DB_ID_18710

* Is Lowered to Limit Found for Type B

Note that some of the VS limits of type D contingencies reported in Table 4-1 and Table 4-2 are higher than those of category B (or C) contingencies, although category D contingencies are generally expected to be more severe. The main reason appears to be that category D contingencies usually cause isolation of part of the system which may contain significant amount of load. Furthermore, the list of category D contingencies is much shorter and may not necessarily include the outages associated with the worst category B (or C) contingencies. These also explain why one of the limits in Table 4-1 was not restricted by any category D contingency until pre-contingency power flow could not converge. As a result, the VS limit of category D was lowered to that of category B, wherever the former was larger than the latter.

4.3 Voltage Stability Comments

The possible transfer increases were expressed in MW rather than percentage to avoid any confusion of the base for percentage, especially in the HWLL2016 scenarios where the sink base changes from generation to load. Moreover, the VS margins (i.e., 5% for single and 2.5% for double/multiple contingencies) were not applied to the created scenarios so that the worst-case scenarios for damping situations were considered. Similarly, the limits might need further reduction due to branch overloads (or even some bus voltage magnitude remaining too low), which were not applied for the same reason. Thus, power flows were created at the possible MW transfer increases (i.e., at the last converged cut-off step) for running SSAT and TSAT.

5. Eigenvalue Analysis

Eigenvalue analysis was performed for several purposes:

- To identify inter-area modes for sensitivity assessment under various system conditions and damping improvement requirements;
- To identify critical local modes that might require damping improvement;
- To determine the critical scenarios for use in PSS tuning;
- To determine the critical contingencies for use in PSS tuning;
- To identify the best PMU locations for oscillation monitoring.

SSAT was run at base power flows, as well as power flows created at the possible Voltage Stability (VS) MW transfer increases, all of them subjected to all type B, C, and D specified contingencies. The results are presented below. Generally, transfers had small effects and HWLL2016 case showed higher damping than FY2018 case. Despite fewer synchronous generators (and thus fewer PSS) in the light load case, the higher damping is consistent with generally milder flows through the network due to lower loading. One inter-area mode and one local mode needed more attention as are discussed below. Note that poorly-damped modes related to the swing generator may show up in some SSAT simulation, which are due to post-contingency overloading of this unit and are not real problems, as confirmed by simply changing the swing bus.

The cases were also checked for all 345 kV single-branch scanned contingencies which did not point to any significantly different results to be reported. Furthermore, the worst type B contingencies were combined with a generator outage, i.e., G-1-1, using either of the following two units:

- The most dominant unit in the reported mode (with no reduction in the corresponding steam unit to capture the worst situation);
- The largest unit in the system.

They did not result in any significantly less damping.

5.1 Peak Load Inter-area Mode Analysis

The inter-area mode results of the peak load analysis are summarized in Table 5-1. Noting that a typical criterion for minimum damping is 3%, all modes appear to be well damped; the lowest damping is 3.7% for type D contingency DB_ID_7804 in Houston transfer, as highlighted in Table 5-1. To further improve the damping of this mode, however, new PSS at two units are recommended. This proposal is based on the Participation Factors (PF) of the mode for the worst scenario, i.e., the Houston transfer.

It will be shown later that tuning of the existing PSS does not improve this mode's damping significantly, as is also evident from the participation entries (i.e., units with significant participation entries do not have PSS). The corresponding Mode Shape (MS) also points to the rather wide-spread nature of the oscillation. The mode shape entries provide a relative measure for how large the oscillation of each unit is on either side of the mode (i.e., positive and negative values). Wide-spread mode shape, where entries taper off gradually, points to inter-area nature of the mode, while a local mode is characterized by one (or a few) large entry and tapering off quickly for the rest of the units.

Table 5-1: FY2018 Lowest-damped Inter-area Modes.

Voltage Stability Transfer	No Fault		Type B Worst Contingency			Type C Worst Contingency			Type D Worst Contingency		
	f (HZ)	ξ (%)	f (HZ)	ξ (%)	Contingency ID	f (HZ)	ξ (%)	Contingency ID	f (HZ)	ξ (%)	Contingency ID
None	0.87	8.23	0.85	7.96	DB_ID_3732	0.78	7.26	DB_ID_2194	0.85	3.91	DB_ID_7804
Houston	0.86	8.68	0.84	8.45	DB_ID_3732	0.79	7.49	DB_ID_2191	**0.85**	**3.70**	**DB_ID_7804**
RGV	0.87	8.52	0.87	8.24	DB_ID_3694	0.72	7.52	DB_ID_2485	0.85	3.94	DB_ID_7804
DFW	0.87	8.13	0.85	7.83	DB_ID_3732	0.78	6.99	DB_ID_2191	0.85	3.92	DB_ID_7804
West	0.87	8.19	0.85	7.91	DB_ID_3732	0.78	7.21	DB_ID_2188	0.85	3.93	DB_ID_7804
Far West	0.87	8.20	0.85	7.92	DB_ID_3732	0.78	7.22	DB_ID_2197	0.85	3.93	DB_ID_7804

5.2 Light Load Inter-area Mode Analysis

The inter-area mode results of the light load analysis are summarized in Table 5-2. The critical mode is the same as that of the peak load case, albeit with somewhat different characteristics and higher damping. This points out that any PSS tuning may be performed on the peak load case.

Table 5-2: HWLL2016 Lowest-damped Inter-area Modes.

Voltage Stability Transfer	No Fault		Type B Worst Contingency			Type C Worst Contingency			Type D Worst Contingency		
	f (HZ)	ξ (%)	f (HZ)	ξ (%)	Contingency ID	f (HZ)	ξ (%)	Contingency ID	f (HZ)	ξ (%)	Contingency ID
None	0.84	9.25	0.84	8.96	DB_ID_14189	0.78	8.21	DB_ID_785	0.72	6.94	DB_ID_7804
Houston	0.80	8.81	0.79	8.61	DB_ID_14134	0.78	8.20	DB_ID_785	0.73	5.01	DB_ID_7804
RGV	0.88	8.80	0.86	8.63	DB_ID_3732	0.76	8.45	DB_ID_2412	0.73	6.68	DB_ID_7804
DFW	0.83	7.44	0.83	7.26	DB_ID_3525	0.79	6.48	DB_ID_785	0.72	6.31	DB_ID_7804
West	0.84	9.07	0.84	8.75	DB_ID_14189	0.78	7.71	DB_ID_785	0.72	6.79	DB_ID_7804
Far West	0.84	9.18	0.84	8.86	DB_ID_14189	0.78	8.03	DB_ID_785	0.72	6.89	DB_ID_7804

5.3 Local Mode Analysis

The local modes of all units appear to be well damped according to SMIB computations. One exception, however, was found under an extreme contingency condition. The results of both peak and light load analyses of this mode are summarized in Table 5-3. Although the mode's frequency falls in the typical inter-area frequency range, it is a local mode dominated by the participations of only two

close plants (which virtually act as one plant), as indicated in the table; it is not an inter-plant mode.

Table 5-3: Local (Two-plant) Mode with Damping Issue Using Full Model.

Voltage Stability Transfer	Type D Contingency DB_ID_12733 in FY2018		Type D Contingency DB_ID_12733 in HWLL2016	
	f (HZ)	ξ (%)	f (HZ)	ξ (%)
None	0.74	-5.59	0.89	0.54
Houston	0.74	-5.62	0.88	0.55
RGV	0.74	-5.63	0.89	0.02
DFW	0.72	-5.36	0.80	-2.05
West	**0.74**	**-5.66**	0.89	0.67
Far West	0.74	-5.61	0.89	0.63

In order to further demonstrate the non-inter-area nature of the above mode, a simplified-model analysis was performed, as well. The simplified model consisted of infinite-bus-behind-reactance models for all non-dominant units, while the units of the two dominant plants were represented with full details. The results are summarized in Table 5-4, which are essentially similar to those of Table 5-3 in post-contingency situations (matching the negative damping magnitude is not important). The pre-contingency results of this table, however, indicate a higher oscillation frequency (in the local or inter-plant frequency range) with much better damping.

Table 5-4: Local (Two-plant) Mode with Damping Issue Using Simplified Model.

Voltage Stability Transfer	FY2018 Case				HWLL2016 Case			
	No Fault		Contingency DB_ID_12733		No Fault		Contingency DB_ID_12733	
	f (HZ)	ξ (%)	f (HZ)	ξ (%)	f (HZ)	ξ (%)	f (HZ)	ξ (%)
None	1.20	4.74	0.71	-10.28	1.27	2.95	0.85	-8.47
Houston	1.21	4.74	0.71	-10.32	1.27	2.95	0.85	-8.48
RGV	1.20	4.73	0.71	-10.32	1.27	2.95	0.85	-8.48
DFW	1.21	5.12	0.70	-10.30	1.27	3.79	0.83	-8.21
West	1.20	4.75	0.71	-10.32	1.27	2.98	0.85	-8.46
Far West	1.20	4.74	0.71	-10.32	1.27	2.94	0.85	-8.47

The above simplified model has the advantage of giving a clue about the frequency of the mode under no-fault condition, which would not otherwise be an easy search. Using this information in the full model, the mode's frequency was in the order of 1.4 Hz with more than 7% damping. In FY2018 case two additional units had a small participation in the mode, as well.

New PSS at the units of two plants are proposed for improving the damping of this mode, as they are the main participating units indicated in Table 5-3. For the worst-case scenario, namely, FY2018 with West transfer and HWLL2016 with DFW transfer, the mode shape entries on both sides (i.e., positive and negative values representing opposite sides of the oscillation) indicate the essentially two-plant nature of the mode; it is not widespread, as the oscillation of the two plants on one side is

counterbalanced by contributions from many other generators in the system. Furthermore, the units involved in this mode have nothing to do with the critical inter-area mode that was discussed above (i.e., the one highlighted in Table 5-1), requiring a completely separate solution. It will also be shown that this mode cannot be significantly improved by tuning the existing PSS.

5.4 Best PMU Locations for Small-signal Stability Monitoring

There are three free-motion eigenvector sets that are traditionally computed and analyzed for each oscillatory mode of interest [2]. They are as follows:

1) Right-eigenvector entries associated with all synchronous generator rotor speed deviations, which are per-unitized using the largest entry as base, with its angle set to zero (i.e., the reference). This vector, also known as Mode Shape (MS), provides a relative measure for the magnitude of the mode that can be seen at each machine rotor, as a result of a small disturbance, irrespective of the disturbance location.
2) Left-eigenvector entries associated with all synchronous generator rotor speed deviations. This vector provides a relative measure for how large the mode can be excited by a small disturbance at the rotor speed of each particular machine, irrespective of the disturbance magnitude.
3) Participation Factor (PF) entries, which are the products of the corresponding entries in the right and left eigenvectors defined above (per-unitized on the largest magnitude thus obtained). The top entries in this vector indicate the best locations for applying Power System Stabilizers (PSS), with the tacit assumption of using speed deviation (or its equivalent as used in PSS2A or similar models) of the machine as the input signal for the PSS compensator.

Based on the above, the best locations for monitoring a mode are those machines with the highest MS entries provided that rotor speed measurement devices are to be used. PMUs, however, are usually located at high-tension buses (rather than generator buses), and the monitoring is associated with the bus voltages (rather than rotor speeds).

Similar to the above, three additional eigenvector sets may be defined that are associated with the bus-voltage magnitude changes, rather than machine speed deviation changes. In particular, the bus Voltage Magnitude Mode Shape (VMMS) is the most appropriate measure to assess the best locations for monitoring a particular mode using PMUs. The vector related to each mode is computed by SSAT for a specified list of buses, which ideally contains all buses in the system. In order to be practical, however, we suggested all 345 kV substations (close to 400 buses in the model) be included in the list and ranked for each mode of interest; lower tension side of the substations may also be used, if applicable. At the end, all ranked lists might be merged into one list of the best substations for monitoring overall system damping using PMUs.

The list in Table 5-5 is selected from the eigenvalue results as modes of interest for this purpose. Modes #1 and #2 are mostly confined to areas 101 [COAST] and 106 [SOUTHERN] and are not that much different. The reason for their slight difference is that they correspond to different contingency categories. In fact, the worst type C contingency is more severe than that of type B, which also results in frequency and damping of mode #2 being less than the corresponding values of mode #1. Mode #3

is mainly contained in area 101 [COAST]. Modes #4, #5, and #6 are the light load versions of modes #1, #2, and #3, respectively.

Table 5-5: Modes of Interest for Monitoring by PMUs.

Mode of Interest for Monitoring by PMUs			Scenario		Contingency	
#	f (HZ)	ξ (%)	Base	Transfer	Type	ID
1	0.85	7.83	FY2018	DFW	B	DB_ID_3732
2	0.78	6.99	FY2018	DFW	C	DB_ID_2191
3	0.85	3.70	FY2018	Houston	D	DB_ID_7804
4	0.83	7.26	HWLL2016	DFW	B	DB_ID_3525
5	0.79	6.48	HWLL2016	DFW	C	DB_ID_785
6	0.73	5.01	HWLL2016	Houston	D	DB_ID_7804

The VMMS results for the top 20 entries, ranked from the largest to the smallest VMMS, of the six modes of interest are listed in Table 5-6 through Table 5-11, respectively.

Table 5-6: Voltage Magnitude Mode Shape Entries for Mode of Interest #1.

VMMS	Bus # [Name]	Area # [Area Name]
1.000	8905 [NEDIN7C 345.]	106 [SOUTHERN]
0.773	80307 [DELSOL7B345.]	106 [SOUTHERN]
0.740	8902 [RIOHONDO345.]	106 [SOUTHERN]
0.563	80355 [DELSOL7A345.]	106 [SOUTHERN]
0.539	5966 [LALTA345345.]	106 [SOUTHERN]
0.454	8317 [LA_PALMA345.]	106 [SOUTHERN]
0.263	80220 [CENIZO7A345.]	106 [SOUTHERN]
0.150	80076 [AJO7A 345.]	106 [SOUTHERN]
-0.216	85000 [N_SHARPE345.]	106 [SOUTHERN]
-0.277	44200 [HILLJE__345.]	101 [COAST]
-0.308	5915 [SO_TEX__345.]	101 [COAST]
-0.365	5725 [PAWNEESW345.]	105 [SOUTH_CE]
-0.374	8455 [LNHILL 6345.]	106 [SOUTHERN]
-0.400	8123 [BLESSING345.]	106 [SOUTHERN]
-0.404	80388 [SDOLLAR7345.]	106 [SOUTHERN]
-0.404	160792 [LBRISAS1345.]	106 [SOUTHERN]
-0.404	160794 [LBRISAS2345.]	106 [SOUTHERN]
-0.440	80382 [NOPALITO345.]	106 [SOUTHERN]
-0.451	8956 [WHITEPT7345.]	106 [SOUTHERN]
-0.685	8164 [COLETO7A345.]	106 [SOUTHERN]

Table 5-7: Voltage Magnitude Mode Shape Entries for Mode of Interest #2.

VMMS	Bus # [Name]	Area # [Area Name]
1.000	8905 [NEDIN7C 345.]	106 [SOUTHERN]
0.767	80307 [DELSOL7B345.]	106 [SOUTHERN]
0.749	8902 [RIOHONDO345.]	106 [SOUTHERN]
0.555	80355 [DELSOL7A345.]	106 [SOUTHERN]
0.539	5966 [LALTA345345.]	106 [SOUTHERN]
0.466	8317 [LA_PALMA345.]	106 [SOUTHERN]
0.266	80220 [CENIZO7A345.]	106 [SOUTHERN]
0.220	160493 [TGW_1_5 345.]	106 [SOUTHERN]
0.220	80071 [ZORILLO7A 345.]	106 [SOUTHERN]
-0.260	8455 [LNHILL 6345.]	106 [SOUTHERN]
-0.288	80388 [SDOLLAR7345.]	106 [SOUTHERN]
-0.288	160794 [LBRISAS2345.]	106 [SOUTHERN]
-0.288	160792 [LBRISAS1345.]	106 [SOUTHERN]
-0.322	8956 [WHITEPT7345.]	106 [SOUTHERN]
-0.323	80382 [NOPALITO345.]	106 [SOUTHERN]
-0.341	44200 [HILLJE__345.]	101 [COAST]
-0.351	5725 [PAWNEESW345.]	105 [SOUTH_CE]
-0.358	5915 [SO_TEX__345.]	101 [COAST]
-0.420	8123 [BLESSING345.]	101 [COAST]
-0.553	8164 [COLETO7A345.]	106 [SOUTHERN]

Table 5-8: Voltage Magnitude Mode Shape Entries for Mode of Interest #3.

VMMS	Bus # [Name]	Area # [Area Name]
1.000	5915 [SO_TEX__345.]	101 [COAST]
0.908	42500 [DOW_____345.]	101 [COAST]
0.560	43035 [OASIS___345.]	101 [COAST]
0.537	43030 [MEADOW__345.]	101 [COAST]
0.392	44000 [W_A_P___345.]	101 [COAST]
0.328	42000 [P_H_R___345.]	101 [COAST]
0.322	44500 [OBRIEN__345.]	101 [COAST]
0.303	47300 [JENETA__345.]	101 [COAST]
0.293	47000 [BELAIR__345.]	101 [COAST]
0.178	110758 [DDPEC_3_345.]	101 [COAST]
0.178	110757 [DDPEC_2_345.]	101 [COAST]
0.178	110756 [DDPEC_1_345.]	101 [COAST]
0.178	40240 [CENTER__345.]	101 [COAST]
0.178	110760 [DDPEC_5_345.]	101 [COAST]
0.178	110759 [DDPEC_4_345.]	101 [COAST]
0.146	40850 [JORDAN__345.]	101 [COAST]
0.138	110076 [CBY4_1_5345.]	101 [COAST]
0.138	40000 [CEDARP__345.]	101 [COAST]
0.136	40255 [CHAMBR__345.]	101 [COAST]
0.136	110737 [BTE_2_5 345.]	101 [COAST]

Table 5-9: Voltage Magnitude Mode Shape Entries for Mode of Interest #4.

VMMS	Bus # [Name]	Area # [Area Name]
1.000	3100 [MARTINLK345.]	102 [EAST]
0.875	3102 [TYLERGND345.]	102 [EAST]
0.872	3109 [STRYKER_345.]	102 [EAST]
0.864	3105 [ELKTON_5345.]	102 [EAST]
0.862	3116 [MTENTRPR345.]	102 [EAST]
0.861	3103 [SHAMBRGR345.]	102 [EAST]
0.852	3119 [NACOGDSE345.]	102 [EAST]
0.835	3117 [LUFKNSS_345.]	102 [EAST]
0.719	40600 [ROANS___345.]	102 [EAST]
0.714	44645 [SNGLTN_3345.]	102 [EAST]
0.689	967 [GIBN_CRE345.]	102 [EAST]
0.639	45972 [KUYDAL75345.]	101 [COAST]
0.620	46500 [TOMBAL__345.]	101 [COAST]
0.594	45971 [KUYDAL74345.]	101 [COAST]
0.584	46290 [RTHWOD__345.]	101 [COAST]
0.584	3130 [FOREGROV345.]	102 [EAST]
0.579	3124 [TRINDAD2345.]	102 [EAST]
0.568	3123 [TRINDAD1345.]	102 [EAST]
0.424	1697 [SULSP_SS345.]	102 [EAST]
0.422	870 [COBISA 345.]	103 [NORTH]

Table 5-10: Voltage Magnitude Mode Shape Entries for Mode of Interest #5.

VMMS	Bus # [Name]	Area # [Area Name]
1.000	3100 [MARTINLK345.]	102 [EAST]
0.874	3116 [MTENTRPR345.]	102 [EAST]
0.856	3119 [NACOGDSE345.]	102 [EAST]
0.851	3102 [TYLERGND345.]	102 [EAST]
0.844	3103 [SHAMBRGR345.]	102 [EAST]
0.843	3105 [ELKTON_5345.]	102 [EAST]
0.839	3109 [STRYKER_345.]	102 [EAST]
0.809	3117 [LUFKNSS_345.]	102 [EAST]
0.584	3130 [FOREGROV345.]	102 [EAST]
0.579	3124 [TRINDAD2345.]	102 [EAST]
0.568	3123 [TRINDAD1345.]	102 [EAST]
0.424	1697 [SULSP_SS345.]	102 [EAST]
0.379	1695 [MOSES_5 345.]	102 [EAST]
-0.187	8905 [NEDIN7C 345.]	106 [SOUTHERN]
-0.191	85000 [N_SHARPE345.]	106 [SOUTHERN]
-0.209	8455 [LNHILL 6345.]	106 [SOUTHERN]
-0.254	44200 [HILLJE__345.]	101 [COAST]
-0.254	42500 [DOW_____345.]	101 [COAST]
-0.255	5915 [SO_TEX__345.]	101 [COAST]
-0.306	8956 [WHITEPT7345.]	106 [SOUTHERN]

Table 5-11: Voltage Magnitude Mode Shape Entries for Mode of Interest #6.

VMMS	Bus # [Name]	Area # [Area Name]
1.000	40600 [ROANS___345.]	102 [EAST]
0.983	44645 [SNGLTN_3345.]	102 [EAST]
0.934	967 [GIBN_CRE345.]	102 [EAST]
0.920	45972 [KUYDAL75345.]	101 [COAST]
0.902	46500 [TOMBAL__345.]	101 [COAST]
0.863	45971 [KUYDAL74345.]	101 [COAST]
0.848	46290 [RTHWOD__345.]	101 [COAST]
0.721	44900 [ZENITH__345.]	101 [COAST]
0.682	44200 [HILLJE__345.]	101 [COAST]
0.681	40900 [KING____345.]	101 [COAST]
0.644	40700 [GRNBYU__345.]	101 [COAST]
0.670	45500 [T_H_W___345.]	101 [COAST]
0.660	46100 [N_BELT__345.]	101 [COAST]
-0.023	80171 [SARITA7A345.]	106 [SOUTHERN]
-0.027	160493 [TGW_1_5 345.]	106 [SOUTHERN]
-0.027	80071 [ZORILLO7345.]	106 [SOUTHERN]
-0.069	85000 [N_SHARPE345.]	106 [SOUTHERN]
-0.088	8956 [WHITEPT7345.]	106 [SOUTHERN]
-0.487	42500 [DOW_____345.]	101 [COAST]
-0.794	5915 [SO_TEX__345.]	101 [COAST]

In order to find the best monitoring buses for all modes, the above tables were combined and sorted in descending order of the absolute values of the VMMS entries. The results are listed in Table 5-12 for the values larger than 0.5. They are within weather areas 101 [COAST], 102 [EAST], and 106 [SOUTHERN]. Service areas that contain these buses are 1 [ONCOR_ED], 4 [CNP_TSP], 8 [AEP_TCC], 10 [STP], 12 [TMPA_TSP], and 15 [BPUB TSP]. ERCOT may choose from this list considering the suitability of the associated substations for PMU installation (or PMU availability at present). In particular, the first four substations provide high observability for all six modes, although inclusion of more locations may be considered to increase the reliability of the monitoring system. Once a location is chosen, however, any nearby bus is redundant and may be skipped. Note that these locations are for monitoring inter-area modes. For local modes the best place is simply the high voltage side of the involved plant.

Table 5-12: Best Monitoring Buses for All Modes of Interest (Ranked).

#	|VMMS|	Bus # [Name]	Weather Area # [Name]	Service Area # [Name]
1	1.000	8905 [NEDIN7C 345.]	106 [SOUTHERN]	8 [AEP_TCC]
2	1.000	5915 [SO_TEX__345.]	101 [COAST]	10 [STP]
3	1.000	3100 [MARTINLK345.]	102 [EAST]	1 [ONCOR_ED]
4	1.000	40600 [ROANS___345.]	102 [EAST]	4 [CNP_TSP]
5	0.983	44645 [SNGLTN_3345.]	102 [EAST]	4 [CNP_TSP]
6	0.934	967 [GIBN_CRE345.]	102 [EAST]	12 [TMPA_TSP]
7	0.920	45972 [KUYDAL75345.]	101 [COAST]	4 [CNP_TSP]

8	0.908	42500 [DOW_____345.]	101 [COAST]	4 [CNP_TSP]
9	0.902	46500 [TOMBAL__345.]	101 [COAST]	4 [CNP_TSP]
10	0.875	3102 [TYLERGND345.]	102 [EAST]	1 [ONCOR_ED]
11	0.874	3116 [MTENTRPR345.]	102 [EAST]	1 [ONCOR_ED]
12	0.872	3109 [STRYKER_345.]	102 [EAST]	1 [ONCOR_ED]
13	0.864	3105 [ELKTON_5345.]	102 [EAST]	1 [ONCOR_ED]
14	0.863	45971 [KUYDAL74345.]	101 [COAST]	4 [CNP_TSP]
15	0.861	3103 [SHAMBRGR345.]	102 [EAST]	1 [ONCOR_ED]
16	0.856	3119 [NACOGDSE345.]	102 [EAST]	1 [ONCOR_ED]
17	0.848	46290 [RTHWOD__345.]	101 [COAST]	4 [CNP_TSP]
18	0.835	3117 [LUFKNSS_345.]	102 [EAST]	1 [ONCOR_ED]
19	0.773	80307 [DELSOL7B345.	106 [SOUTHERN]	8 [AEP_TCC]
20	0.749	8902 [RIOHONDO345.]	106 [SOUTHERN]	8 [AEP_TCC]
21	0.721	44900 [ZENITH__345.]	101 [COAST]	4 [CNP_TSP]
22	0.685	8164 [COLETO7A345.]	106 [SOUTHERN]	8 [AEP_TCC]
23	0.682	44200 [HILLJE__345.]	101 [COAST]	4 [CNP_TSP]
24	0.681	40900 [KING____345.]	101 [COAST]	4 [CNP_TSP]
25	0.670	45500 [T_H_W___345.]	101 [COAST]	4 [CNP_TSP]
26	0.660	46100 [N_BELT__345.]	101 [COAST]	4 [CNP_TSP]
27	0.644	40700 [GRNBYU__345.]	101 [COAST]	4 [CNP_TSP]
28	0.584	3130 [FOREGROV345.]	102 [EAST]	1 [ONCOR_ED]
29	0.579	3124 [TRINDAD2345.]	102 [EAST]	1 [ONCOR_ED]
30	0.568	3123 [TRINDAD1345.]	102 [EAST]	1 [ONCOR_ED]
31	0.563	80355 [DELSOL7A345.	106 [SOUTHERN]	8 [AEP_TCC]
32	0.560	43035 [OASIS___345.]	101 [COAST]	4 [CNP_TSP]
33	0.539	5966 [LALTA345345.	106 [SOUTHERN]	15 [BPUB TSP]
34	0.537	43030 [MEADOW__345.]	101 [COAST]	4 [CNP_TSP]

5.5 Load Model Sensitivity

It is well known that load models can have a significant effect on damping. In general, moving from constant impedance to constant power model (i.e., stiffer load) is expected to reduce damping, while the active power component has a larger effect than the reactive component. Furthermore, loads usually contain a significant amount of induction motors of various sizes. The critical modes were reproduced using the following two variations to assess the eigenvalue sensitivity to load models:

1) Stiffening the active component of all loads to 100% constant current and the reactive component to 50% constant power and 50% constant current models.
2) Converting 20% of all loads to Small Motors (SM) using a complex load (CLODAL) model.

A comparison of the critical modes under the studied load model characteristics is presented in Table 5-13. It can be seen that the damping reductions for both the stiffer static load models and those with

dynamic contents may be significant but are not critical (and will be insignificant after adding the recommended PSS).

Table 5-13: Sensitivity of Critical Modes to Load Models.

Mode Description	Loading	Transfer	PL: 50%I, 50%Z QL: 50%P, 50%Z		PL: 100%I QL: 50%P, 50%I		PL: 20%SM, 80%I QL: 20%SM, 80%Z	
			f (HZ)	ξ (%)	f (HZ)	ξ (%)	f (HZ)	ξ (%)
Inter-area Mode after Type D Contingency DB_ID_7804	FY2108	Houston	0.85	3.70	0.85	3.43	0.83	3.28
	HWLL2016	Houston	0.73	5.01	0.73	5.66	0.70	5.78
Two-plant Mode after Type D Contingency DB_ID_12733	FY2108	West	0.74	-5.66	0.73	-6.22	0.74	-7.18
	HWLL2016	DFW	0.80	-2.05	0.80	-2.34	0.79	-1.16

5.6 Wind Generation Dynamics Impact

In order to assess the dynamics impact of the wind generation, the critical modes were recalculated after removing all dynamic models of wind generators. This was accomplished through the dynamic representation capability in SSAT in two different ways as follows:

1) All corresponding units were netted out (i.e. 2332 MW and 8574 MW in the peak and light load base cases, respectively). Note that generation netting is a negative constant-impedance load representation, which is quite soft from a damping point of view.
2) Each corresponding unit was replaced by an infinite bus behind its source impedance. Note that this model is a simplified (no dynamics) equivalent for synchronous generator representation, which may be stiffer than netting in some situations.

As the comparisons of Table 5-14 show, such representations do not impact the critical eigenvalues in any meaningful way (and will be quite insignificant after adding the recommended PSS). In other words, the impact of wind farm dynamics is more or less neutral as far as the low-frequency oscillation damping is concerned. This also makes theoretical sense because most of the wind generations are interfaced to the system with power electronics that operate based on fast controls.

Table 5-14: Wind Generation Impact on Critical Modes.

Mode Description	Loading	Transfer	Dynamic Wind Generator Models		Netted Wind Generator Models		Infinite-bus wind Generator Models	
			f (HZ)	ξ (%)	f (HZ)	ξ (%)	f (HZ)	ξ (%)
Inter-area Mode after Type D Contingency DB_ID_7804	FY2108	Houston	0.85	3.70	0.85	3.70	0.85	3.73
	HWLL2016	Houston	0.73	5.01	0.73	4.93	0.78	4.92
Two-plant Mode after Type D Contingency DB_ID_12733	FY2108	West	0.74	-5.66	0.74	-5.65	0.74	-3.79
	HWLL2016	DFW	0.80	-2.05	0.80	-2.40	0.81	-4.63

5.7 Time-domain Verifications

Before proceeding to the PSS tuning, the eigenvalue analysis results were verified by time-domain simulations. This is important in order to fully validate and understand the basic characteristics of the critical modes (frequency, damping, mode shape, etc.) produced by eigenvalue analysis.

The verification of critical modes was performed for all scenarios. However, since transfers had little effect on the critical modes and light load offered better damping, mostly the worst peak load scenarios are presented here for small disturbances (i.e., exciting the critical modes) as follows:

- Type D contingency DB_ID_7804 in the Houston transfer of FY2018 as pre-contingency, and then at 0.1 second a 3-phase fault applied for 3 time steps (i.e., 0.012 second) with no subsequent tripping.
- Type D contingency DB_ID_12733 in the West transfer of FY2018 as pre-contingency, and then at 0.1 second a 3-phase fault applied for 3 time steps (i.e., 0.012 second) with no subsequent tripping.

The simulation results are plotted in Figure 5-1 and Figure 5-2, respectively. In each figure the relative rotor angles of the most dominant unit and the unit with the highest mode shape entry on the opposite side are plotted. In such a selected signal pair, the corresponding mode is very observable (i.e., high magnitude) and oscillates in almost opposite phase angles, confirming the mode shape characteristics found in eigenvalue analysis.

To further compare the time-domain simulations and eigenvalue results, Prony analysis was performed on the relative rotor angle signals of the most dominant generator in both peak and light load scenarios (i.e., the black curves in Figure 5-1 and Figure 5-2). The results are compared with those of eigenvalue analysis in Table 5-15, which show good consistency on the mode frequencies and damping ratios found by the two different analysis approaches. Note that Prony analysis results can vary depending on the fault location/severity, analyzed signal, and analyzed window span. As a result, it is considered less reliable than eigenvalue analysis.

Table 5-15: Mode Comparisons of the Existing System.

Mode Description	Loading	Transfer	Eigenvalue Analysis		Prony Analysis	
			f (HZ)	ξ (%)	f (HZ)	ξ (%)
Inter-area Mode after Type D Contingency DB_ID_7804	FY2108	Houston	0.85	3.70	0.85	4.56
	HWLL2016	Houston	0.73	5.01	0.74	6.21
Two-plant Mode after Type D Contingency DB_ID_12733	FY2108	West	0.74	-5.66	0.66	-3.78
	HWLL2016	DFW	0.80	-2.05	0.80	-1.26

Verification of the best PMU locations was performed by comparing the voltage responses of the buses having 1.0 PU VMMS (i.e., the highest amplitude) with their corresponding ones having the lowest VMMS absolute values. As a result, the buses to be compared in each loading condition are those listed in Table 5-16. The comparison should more or less hold in all situations, and thus should

be performed irrespective of the transfers and contingencies.

Table 5-16: Suggested Buses for Oscillation Monitoring Comparisons.

Description	Buses with 1.0 PU |VMMS|	Buses with the Lowest |VMMS|
FY2018 Scenarios	First Bus at the Top Tail Second Bus at the Top Tail	First Bus at the Bottom Tail Second Bus at the Bottom Tail
HWLL2016 Scenarios	First Bus at the Top Tail Second Bus at the Top Tail	First Bus at the Bottom Tail Second Bus at the Bottom Tail

For this purpose, both loading conditions are subjected to a large disturbance. The simulation results are plotted in Figure 5-3 and Figure 5-4, for the base peak and light load scenarios, respectively. In each figure the voltage magnitudes of the associated buses in Table 5-16 are plotted. The plots clearly show high contents of oscillatory modes for the buses with 1.0 PU VMMS, and low contents for the opposite buses. It may also be noted that the two plots of the low VMMS buses in HWLL2016 case are virtually the same, which is consistent with the eigenvalue analysis indicating virtually equal |VMMS| values for them.

In conclusion, the non-linear time-domain simulation verifications prove that the linearized eigenvalue analysis approach is able to correctly find the oscillatory modes in the system with sufficiently accurate characteristics, which also points to robustness of the two-complementary-analyses approach used in this project.

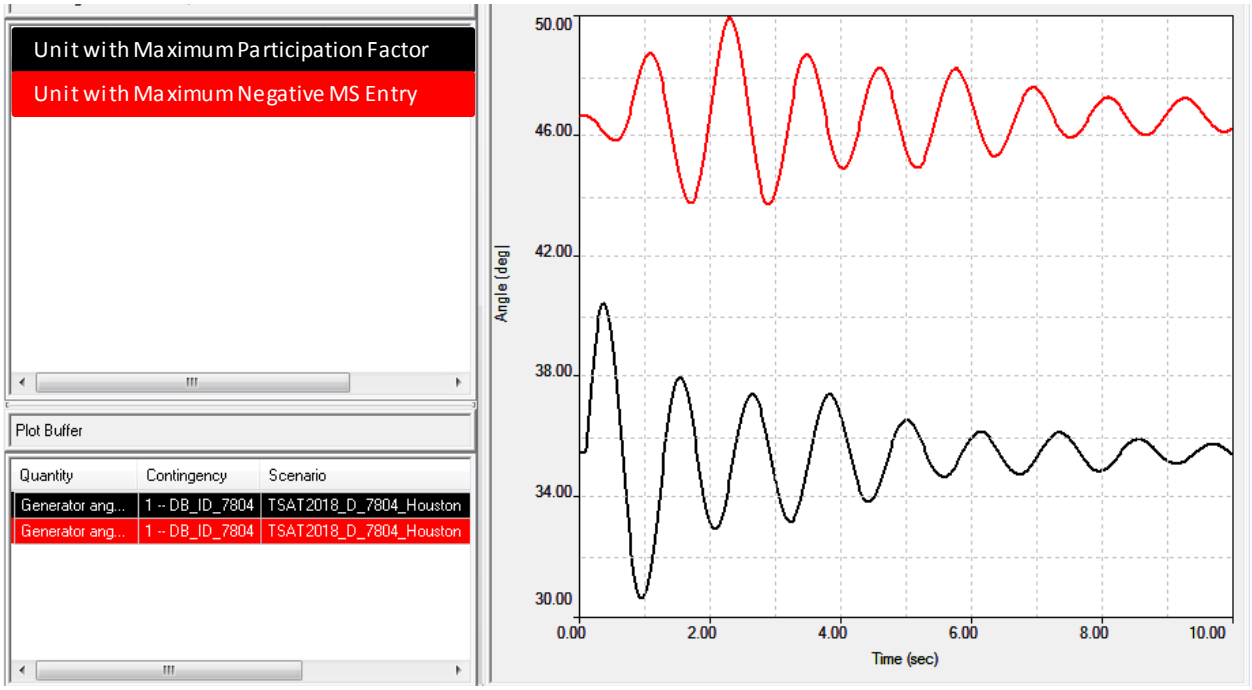

Figure 5-1: Small-disturbance Time-domain Responses for the Critical Inter-area Mode.

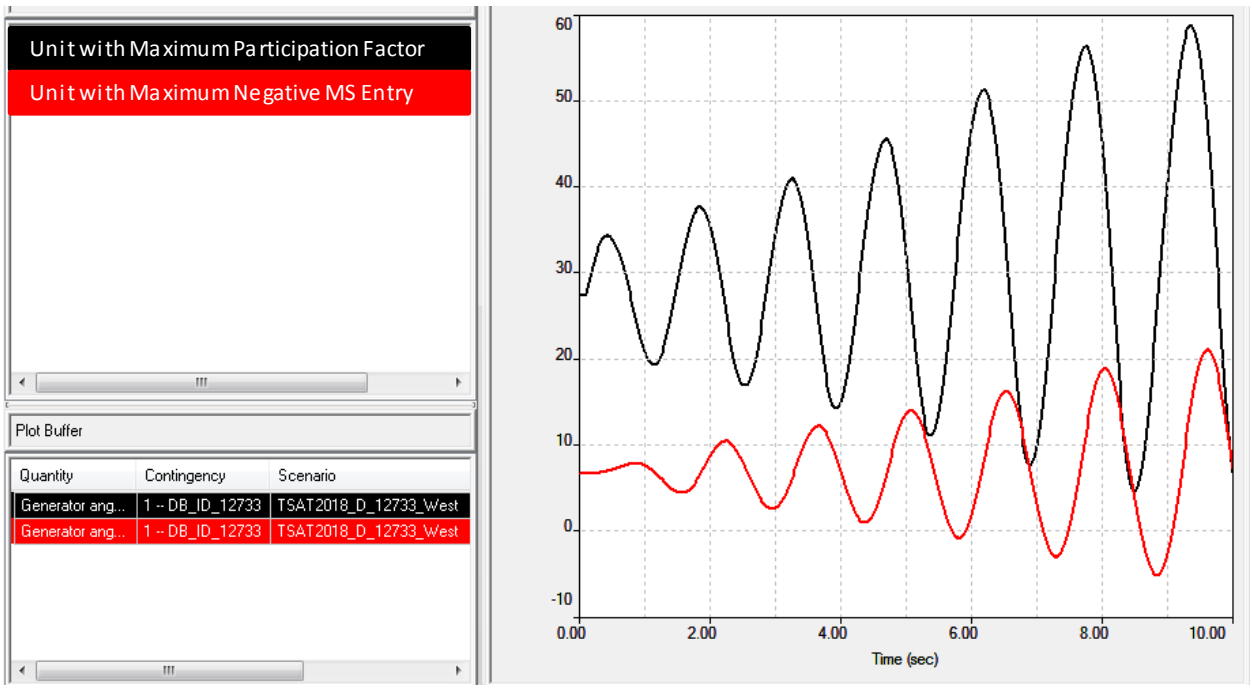

Figure 5-2: Small-disturbance Time-domain Responses for the Critical Local (Two-plant) Mode.

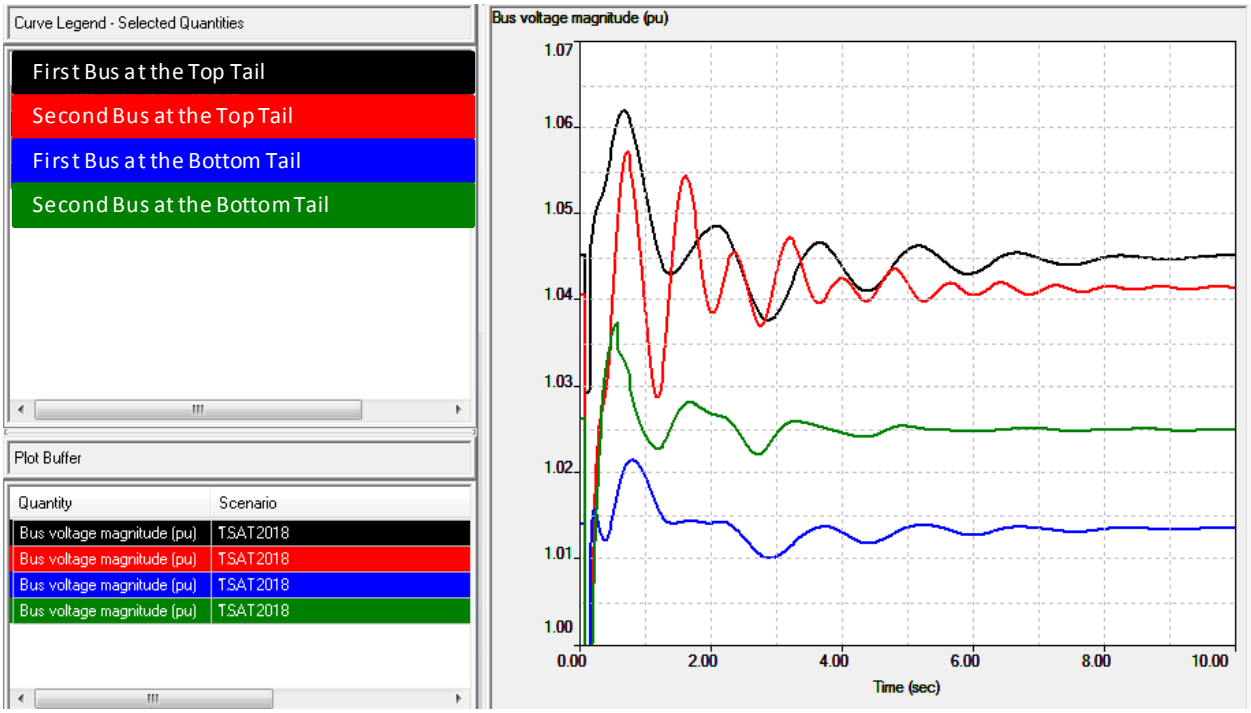

Figure 5-3: FY2018 Large-disturbance Simulation Results for Oscillation Monitoring.

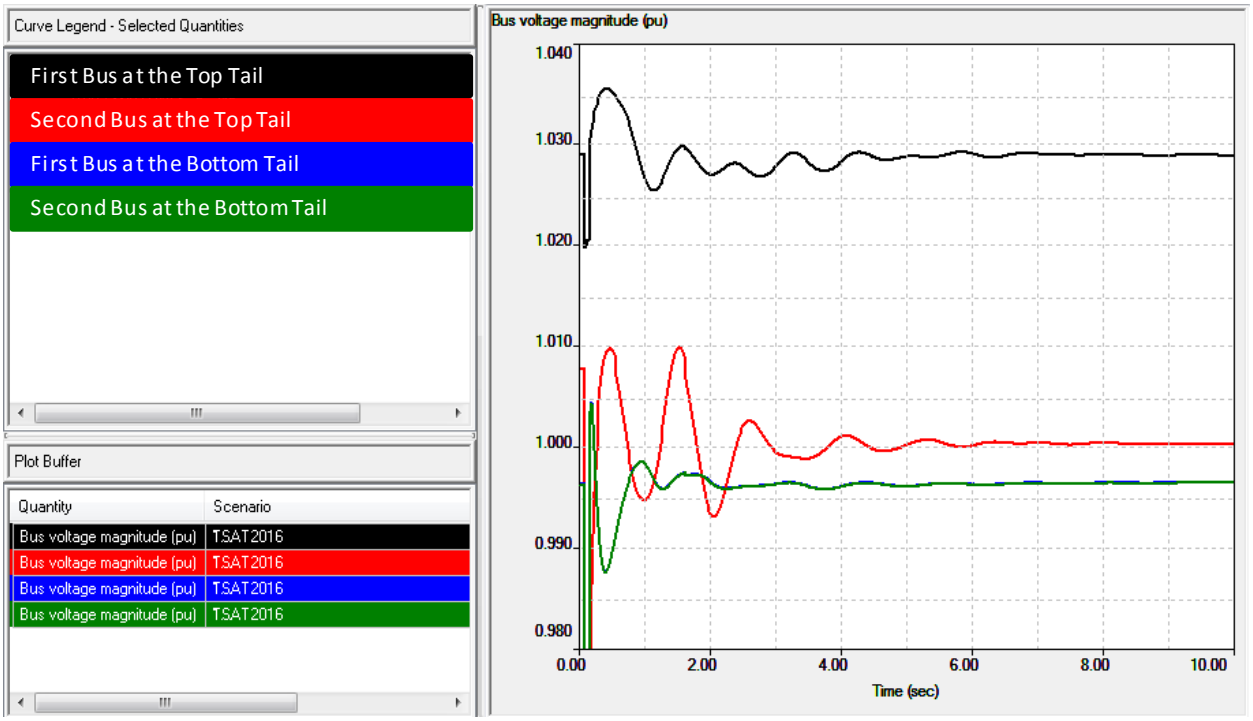

Figure 5-4: HWLL2016 Large-disturbance Simulation Results for Oscillation Monitoring.

6. Tuning of Power System Stabilizers

Tuning was performed for the existing and newly proposed PSS. They are discussed below along with the tuning procedure. References [2] and [5] contain useful information on the theoretical background of the control device tuning for damping enhancement.

6.1 Tuning Procedure

PSS is tuned to improve both local and inter-area mode damping, while in large interconnected systems the emphasis is usually on the latter. Three sets of parameters may be tuned in a small-signal stability study:

1) Washout time constant (and related parameters).
2) Phase compensation.
3) Gain setting.

For other parameters of PSS typical values are commonly used. They include the following:

- *Torsional filter:* When PSS has a torsional filter, the corresponding parameters are selected to suppress the content of torsional modes in the generator speed deviation input. Tuning of these parameters requires detailed generator multi-mass shaft dynamic model (inertia for individual shaft masses and the spring effect coefficients between masses). Since the parameters of a torsional filter do not depend on system operating conditions, they should be valid once tuned appropriately, unless the generator hardware is modified.
- *Stabilizer output limiter:* The stabilizer output limiter is usually set in accordance with other protective devices of the generator, such as terminal voltage limiter [2]. Therefore, tuning the limiter parameters requires the information of these protective devices. Field testing might also be required to ensure that the settings are adequately coordinated.

The tunings of this study were performed using PLI's Control Design Toolbox (CDT) which is interfaced to SSAT. The associated steps are described below.

6.1.1 Washout Time Constant

Washout is a high-pass filter that prevents steady change in the input signal from modifying field voltage; Figure 6-1 shows its frequency-domain characteristics for various time constants. The value of the washout time constant should be long enough to allow signals of the frequencies of interest to pass without significant attenuation, but not so long that the PSS responds to system wide frequency variations, as well as amplifying noise.

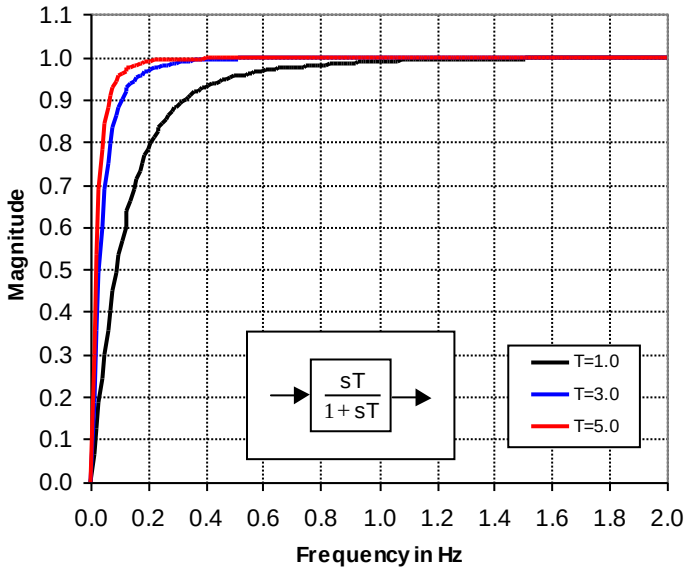

Figure 6-1: Frequency Characteristics of Washout Functions.

From the viewpoint of the washout function, the precise value of the washout time constant is not critical and is typically chosen to be between 1 and 5 seconds (or even longer). A "rule of thumb" is to ensure that the magnitude of the washout function is greater than 98% for the entire frequency range of interest.

When the second input signal of PSS2A and PSS2B models is electrical power, the K_{S2}/T_7 block is actually a combination of integrator and washout functions as shown in Figure 6-2, where T7 should match the other washout time constants. In this case, K_{S2}/T_7 in the integrator part should be set to 1/2H where H is the inertia constant of the generator due to the fact that the torsional filter input is supposed to be the synthesized mechanical power [2]. Therefore, $K_{S2} = 0.5\ T_7 / H$, while $K_{S3} = 1$.

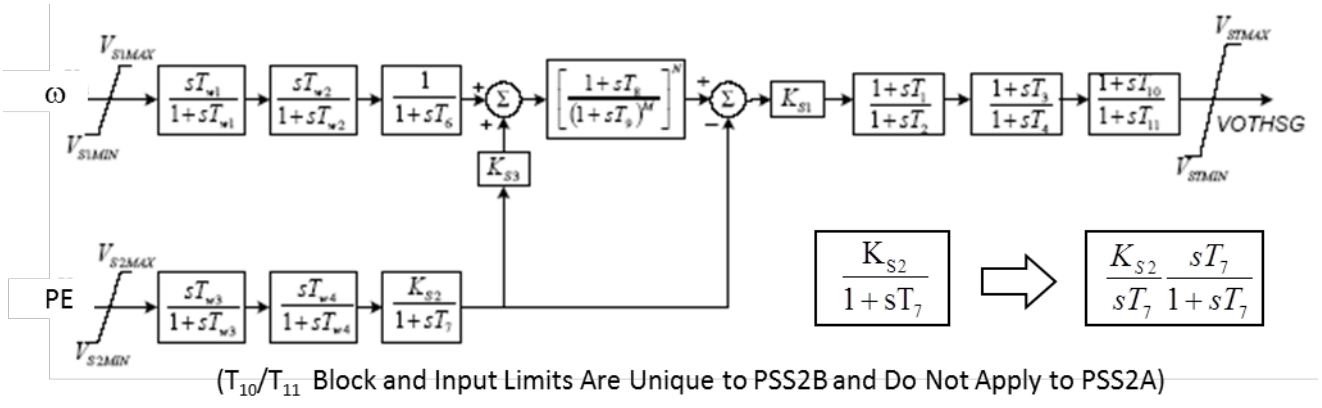

Figure 6-2: K_{S2}/T_7 Block of the PSS2A and PSS2B Models with Speed and Power Inputs.

6.1.2 Phase Compensation

Time constants of the lead/lag blocks of a PSS are tuned using the frequency response approach. The idea is to introduce an appropriate phase lead by the PSS to compensate the phase lag between the exciter Automatic Voltage Regulator (AVR) reference junction and the machine air-gap torque. As shown in [2], this increases the damping component of the torque delivered by the generator, and thus, adds damping to the modes of oscillations. The phase compensation for a PSS can be determined using the following two sub-steps:

1) *Compute the phase characteristics between the exciter AVR reference and the air-gap torque over the required frequency range.* These characteristics do not significantly change with network details, and thus, an SMIB model is usually sufficient. Note that the effect of the feedback from the generator rotor angle should be excluded (i.e., open loop frequency response). This can be done by using a large value for machine inertia to hold the rotor angle constant. Normally, increasing H by 500 to 1000 times is sufficient for this purpose.

2) *Determine the appropriate phase compensation by PSS. PSS usually contains two, or sometime three, lead/lag blocks to provide phase compensation.* Each lead/lag block can theoretically provide up to 90 degrees phase angle, but practically the maximum should not exceed 60 degrees. Lead/lag blocks also affect the gain as shown in the example of Figure 6-3. When determining the actual phase compensation, it is advised to always under-compensate the phase lag computed from the generator, i.e., the phase lead to be provided by the PSS should be less than the phase lag between the exciter AVR reference and the air-gap torque. This is to ensure that the PSS provides considerable damping torque while not adversely affecting the synchronizing torque. With this rule, the more the phase lag is compensated, the more the damping is improved.

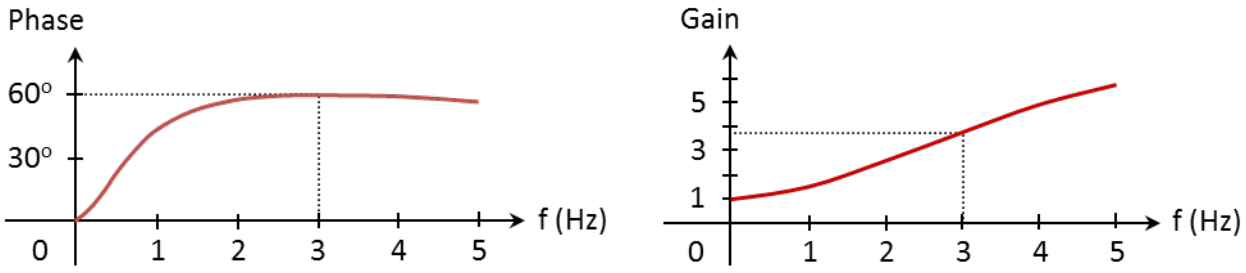

Figure 6-3: Example of a Lead Function Providing Maximum 60 Degrees at 3 Hz.

An example of phase compensation is provided in Figure 6-4. Another factor to consider when determining the phase compensation is the phase characteristics of the other functions in the PSS. For example, washout function adds a small phase lead in the low frequency range, and when the washout time constant is small (say, less than 1 second), this phase lead may be significant for very low frequency inter-area modes.

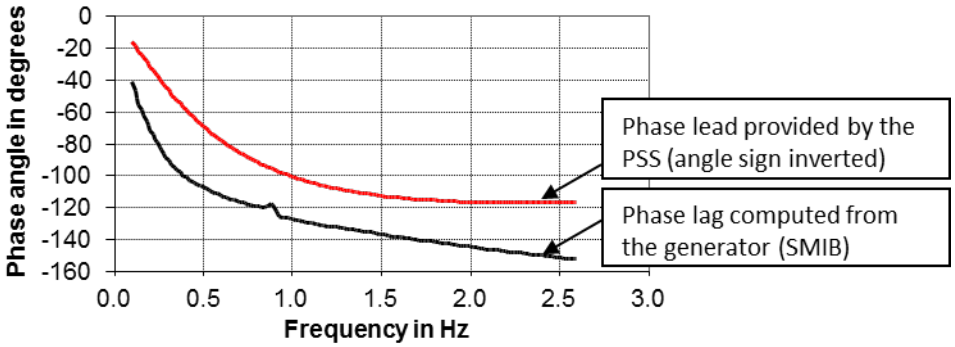

Figure 6-4: Example of PSS Phase Compensation Design.

6.1.3 Gain Setting

The PSS gains are determined using a combination of two approaches as follows:

1) *Root locus*: The critical mode is computed at different gains and an optimal gain is selected in terms of the improvement it provides on the damping. An example is presented in Figure 6-5, which indicates that the damping of the mode is maximized at a gain of about 15, after which the damping decreases again and may even become negative at larger gains. Therefore, the gain of this PSS should not be set at a value larger than 15. It needs to be done for all modes (including control modes) and the final gain selection should assure sufficient margin for all circumstances.
2) *Time-domain simulation*: This is to ensure that the PSS output signal does not remain saturated for a long time after major disturbances. The gain found by root locus may need to be further reduced due to this reason.

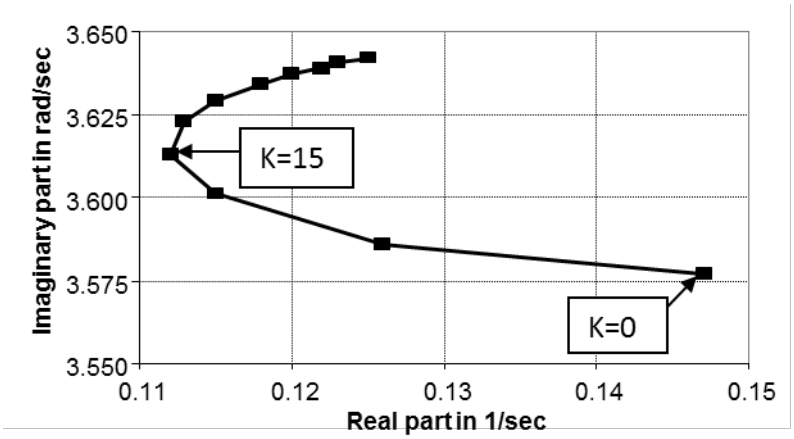

Figure 6-5: Root Locus Example.

6.2 Tuning of the New PSS

PSS are proposed for two units to improve the critical inter-area mode, as well as for the units of two plants to improve the critical local mode. PSS2A model is assumed for all newly proposed PSS. Their washout time constants are set at 2.0 seconds and their limits at ±0.05, with typical torsional filter parameters.

The phase compensation plots of the proposed PSS for the critical inter-area mode damping improvement are presented in Figure 6-6 (similar for the other unit of the same plant). The computations are performed for the Houston transfer of the peak load with DB_ID_7804 type D contingency (i.e., the worst-case condition for the mode in question). Gain tuning by CDT indicated no restriction for K_{S1} (checked from 0.1 to 30 in steps of 1.0).

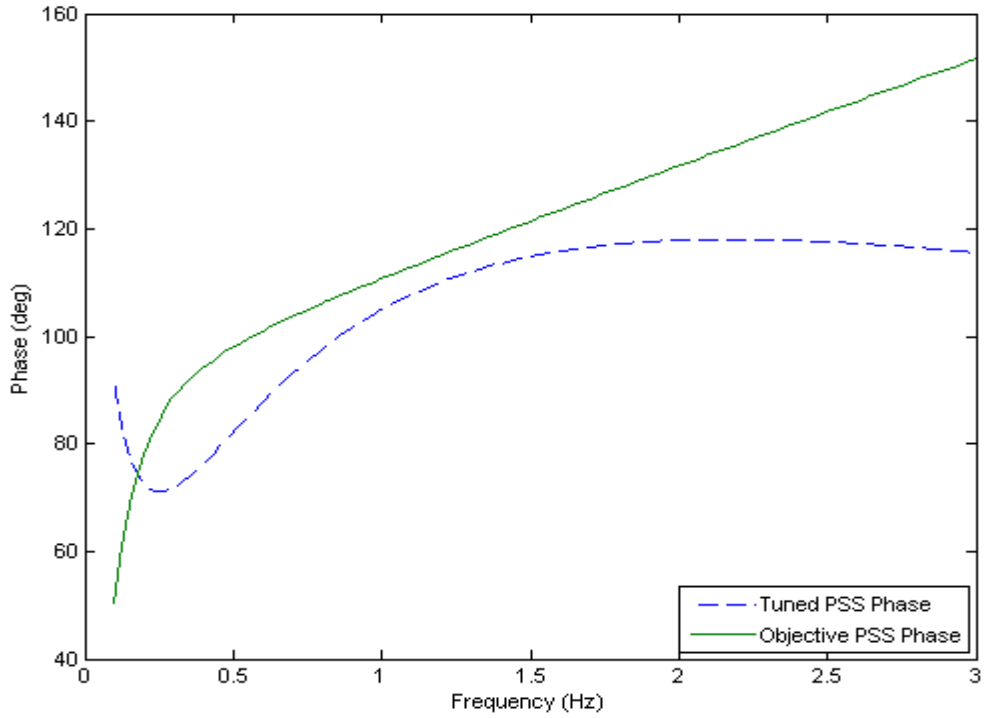

Figure 6-6: PSS Phase Compensation for a Unit Corresponding to the Critical Inter-area Mode.

The phase compensation plots of the proposed PSS for the critical local (two-plant) mode damping improvement are presented in Figure 6-7 and Figure 6-8 (not much different for the units of the same plant). The computations are performed for the West transfer peak load with DB_ID_12733 type D contingency (i.e., the worst case condition for the mode in question). Gain tuning by CDT indicated no restriction for K_{S1} (checked from 0.1 to 30 in steps of 1.0).

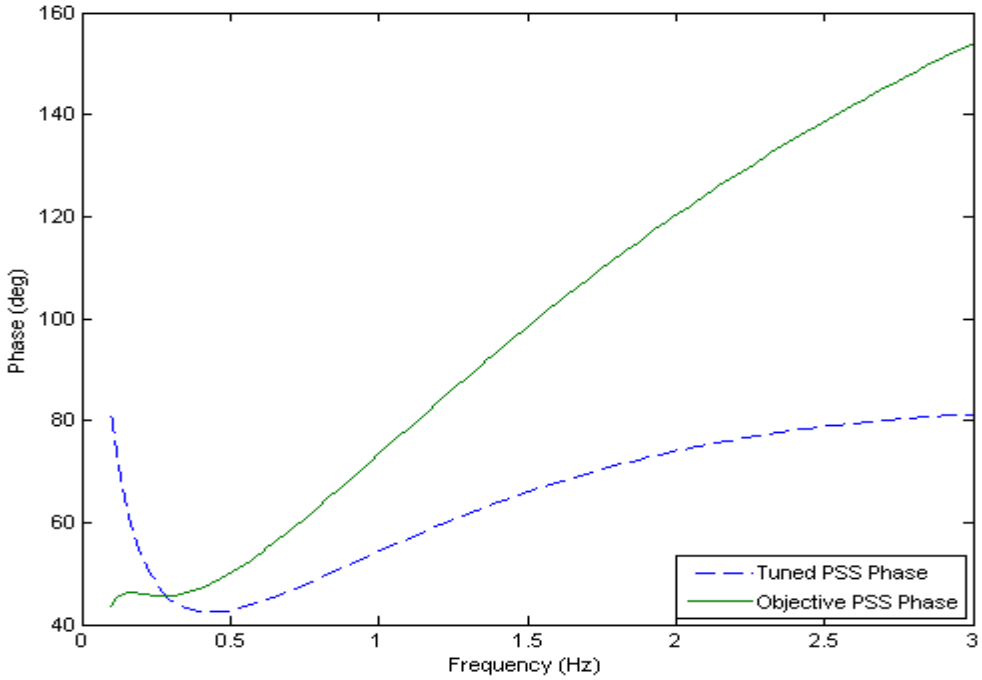

Figure 6-7: PSS Phase Compensation for a Unit of Plant 1 Corresponding to the Critical Local Mode.

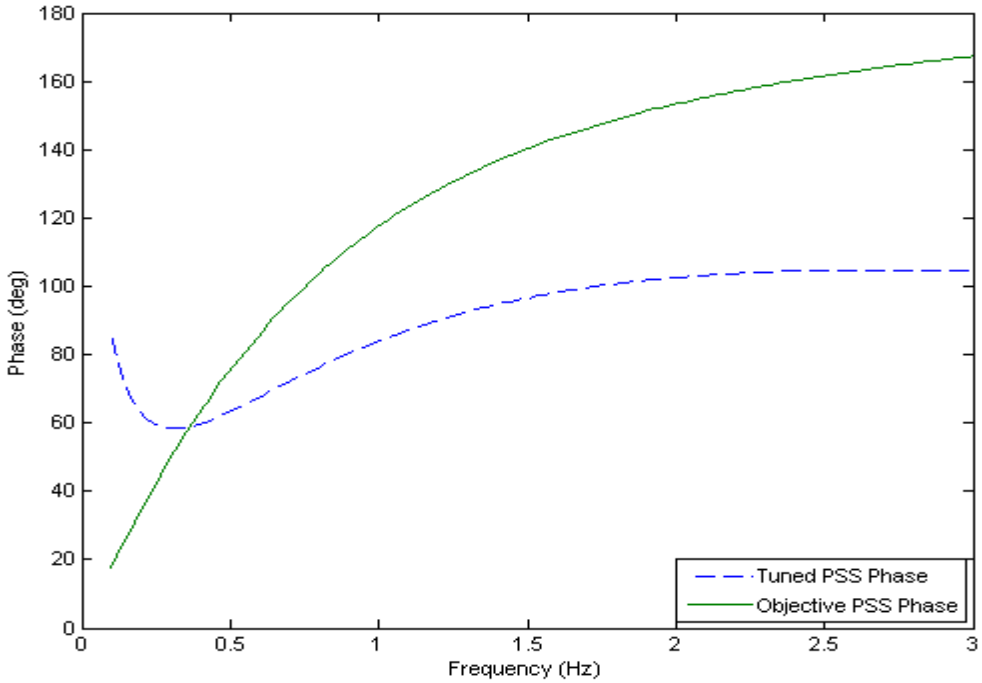

Figure 6-8: PSS Phase Compensation for a Unit of Plant 2 Corresponding to the Critical Local Mode.

Considering that the PSS gain should not be increased after it fulfils the required damping improvement (i.e., to avoid adverse effects on other modes), and should not show sustained output saturation in time-domain simulations (discussed later in this section), the final data for all newly proposed PSS (in PSS/E format) are as follows:

6.3 Tuning of the Existing PSS

There were 116 PSS2A, 25 PSS2B, 22 IEEEST, and 1 ST2CUT (i.e., a total of 164) in-service PSS models in FY2018 case, all of which were examined. Note that the HWLL2016 case contained essentially the same PSS set, but with 108 of them being out of service. Thus, examining the peak load PSS was sufficient. The results, indicated that K_{s2} gain was wrongly set in a number of PSS, as reported in Table 6-1 along with their correct settings. Note that this setting mainly affects the torsional filtering performance and not the low frequency damping. The washout time constants, as well as other parameters, appeared to be within their corresponding typical ranges.

Table 6-1: Suggested PSS Parameter Corrections.

#	PSS Model	Existing K_{S2}	Suggested $K_{S2} = T_7/2H$
1	PSS2A	0.250	0.203
2	PSS2A	0.213	0.284
3	PSS2A	1.992	1.748
4	PSS2A	0.368	0.503
5	PSS2A	0.368	1.042
6	PSS2B	1.170	1.805
7	PSS2B	0.172	0.344
8	PSS2A	1.900	2.119
9	PSS2A	0.200	0.133
10	PSS2A	0.200	0.133
11	PSS2A	0.200	0.133
12	PSS2A	0.200	0.133
13	PSS2A	0.200	0.133
14	PSS2A	0.200	0.133
15	PSS2A	0.150	0.187
16	PSS2A	0.150	0.187
17	PSS2A	0.744	0.317
18	PSS2A	0.522	1.037
19	PSS2A	0.200	0.133
20	PSS2A	0.200	0.133
21	PSS2A	0.200	0.133
22	PSS2A	0.200	0.133
23	PSS2B	0.389	0.446

As was concluded earlier, the transfer scenarios and contingencies did not produce any situation that existing PSS tuning might either be required or have a significant effect for the extreme situations

showing low damping; new PSS were needed for the damping improvement requirements. Similarly, the light load case showed better damping in all studied situations. Thus, the phase compensation tuning was performed for all PSS2A and PSS2B models in FY2018 base case using CDT. Note that older types of PSS models (i.e., IEEEST and ST2CUT) were sanity checked but not tuned; they had no apparent issue.

The results of phase compensation tuning show that tuned parameters offer very little improvement for most of the PSS, which may be left intact. On the other hand, a number of them indicate significant over-compensation, as well as under-compensation, in the frequency range of interest. These are listed in Table 6-2, for which field implementation of the tunings is suggested.

Table 6-2: Suggested PSS Phase Tunings.

#	PSS Model	Existing T_1, T_2, T_3, T_4, T_{10}, T_{11}	Suggested T_1, T_2, T_3, T_4, T_{10}, T_{11}
1	PSS2A	0.306, 0.083, 0.306, 0.083	0.146, 0.020, 0.146, 0.020
2	PSS2A	0.150, 0.030, 0.150, 0.030	0.292, 0.020, 0.292, 0.020
3	PSS2A	0.150, 0.030, 0.150, 0.030	0.292, 0.020, 0.292, 0.020
4	PSS2A	0.100, 0.040, 0.270, 0.030	0.279, 0.020, 0.156, 0.020
5	PSS2A	0.150, 0.030, 0.150, 0.030	0.091, 0.020, 0.091, 0.020
6	PSS2B	0.200, 0.035, 0.200, 0.035, 0.200, 0.035	0.082, 0.020, 0.212, 0.020, 0.082, 0.020
7	PSS2B	0.280, 0.040, 0.360, 0.040, 0.440, 0.600	0.127, 0.020, 0.127, 0.020, 0.127, 0.020
8	PSS2A	0.150, 0.050, 0.150, 0.025	0.107, 0.020, 0.216, 0.020
9	PSS2A	0.200, 0.040, 0.360, 0.120	0.279, 0.020, 0.070, 0.020
10	PSS2A	0.200, 0.040, 0.360, 0.120	0.279, 0.020, 0.070, 0.020
11	PSS2A	0.200, 0.040, 0.360, 0.120	0.279, 0.020, 0.069, 0.020
12	PSS2A	0.200, 0.040, 0.360, 0.120	0.279, 0.020, 0.069, 0.020
13	PSS2A	0.200, 0.040, 0.360, 0.120	0.279, 0.020, 0.069, 0.020
14	PSS2A	0.200, 0.040, 0.360, 0.120	0.279, 0.020, 0.069, 0.020
15	PSS2A	0.140, 0.035, 0.140, 0.035	0.183, 0.020, 0.183, 0.020
16	PSS2A	0.140, 0.035, 0.140, 0.035	0.183, 0.020, 0.183, 0.020
17	PSS2A	0.140, 0.035, 0.140, 0.035	0.184, 0.020, 0.184, 0.020
18	PSS2B	0.100, 0.020, 0.100, 0.020, 0.300, 0.030	0.172, 0.020, 0.172, 0.020, 0.172, 0.500
19	PSS2A	0.340, 0.020, 0.340, 0.020	0.148, 0.020, 0.148, 0.020
20	PSS2A	0.340, 0.020, 0.340, 0.020	0.148, 0.020, 0.148, 0.020
21	PSS2A	0.340, 0.020, 0.340, 0.020	0.148, 0.020, 0.148, 0.020
22	PSS2A	0.340, 0.020, 0.340, 0.020	0.148, 0.020, 0.148, 0.020
23	PSS2A	0.200, 0.040, 0.360, 0.120	0.274, 0.020, 0.068, 0.020
24	PSS2A	0.200, 0.040, 0.360, 0.120	0.274, 0.020, 0.068, 0.020
25	PSS2A	0.200, 0.040, 0.360, 0.120	0.274, 0.020, 0.068, 0.020
26	PSS2A	0.200, 0.040, 0.360, 0.120	0.274, 0.020, 0.068, 0.020
27	PSS2B	0.240, 0.040, 0.240, 0.040, 0.100, 0.100	0.099, 0.020, 0.099, 0.020, 0.099, 0.020

Gain tuning was also performed for all PSS2A and PSS2B models in FY2018 base case using CDT. A few PSS showed insufficient margin for avoiding possible control mode instabilities. They are listed in Table 6-3, along with their suggested reduced gains.

Table 6-3: Suggested PSS Gain Tunings.

#	PSS Model	Existing K_{S1}	Suggested K_{S1}
1	PSS2B	15.0	13.0
2	PSS2A	15.0	9.0
3	PSS2B	15.0	10.0
4	PSS2B	15.0	10.0
5	PSS2B	15.0	10.0
6	PSS2B	15.0	10.0

6.4 Performance of the New PSS

The new PSS performances were checked using both SSAT and TSAT. The modal results of the worst-case scenarios, namely, DB_ID_7804 contingency in the Houston transfer of FY2018 and DB_ID_12733 contingency in the West transfer of FY2018, are presented in Table 6-4. The applied TSAT small-disturbances are the same as those of previous section. Eigenvalue and time-domain simulations are in close agreement and both indicate adequate damping provided by the newly added PSS. Time-domain plots of the most dominant units of these modes, with and without the new PSS, are also compared in Figure 6-9 and Figure 6-10.

It should be noted that tuning of the existing PSS has shown insignificant effect on the two critical modes, and therefore such results are not presented; they offer other improvements that are discussed later in this section. Similarly, the new PSS intended for each of the modes in Table 6-4 has virtually had no effect on the other mode. Moreover, after adding the recommended PSS neither the damping reductions for more severe load models nor the impact of the wind generation had any significance to be reported, as all damping ratios remained well above what may be required in practice.

Table 6-4: Mode Comparisons for New PSS Performance.

Description	Eigenvalue Analysis				Prony Analysis			
	Without New PSS		With New PSS		Without New PSS		With New PSS	
	f (HZ)	ξ (%)	f (HZ)	ξ (%)	f (HZ)	ξ (%)	f (HZ)	ξ (%)
Inter-area Mode after Type D Contingency DB_ID_7804 in the FY2018 Houston Transfer	0.85	3.7	0.84	6.20	0.85	4.56	0.85	6.73
Two-plant Mode after Type D Contingency DB_ID_12733 in the FY2018 West Transfer	0.74	-5.66	0.75	6.33	0.66	-3.78	0.75	6.18

In order to check the new PSS gain and limits, two large disturbances (#1 and #2) were simulated in TSAT. The outputs of the new PSS are plotted in Figure 6-11 and Figure 6-12, which indicate the proper setting of their gains. Note that their limits were set at moderate values and there seems to be no need for their further widening. Furthermore, the active power outputs of the units with and without the proposed PSS are compared in Figure 6-13 and Figure 6-14, which indicate that the new PSS also provide some reduction in the first-swing peak-to-peak power oscillations. Furthermore, the power oscillations subside in a much less duration as a result of the new PSS.

Note that the associated exciters of the proposed PSS, having EXAC1, IEEET2, and EXST1 models, all appear to be fast and appropriate, as far as the PSS are concerned. Moreover, exciter step responses of TSAT did not show any slowness associated with these exciters either.

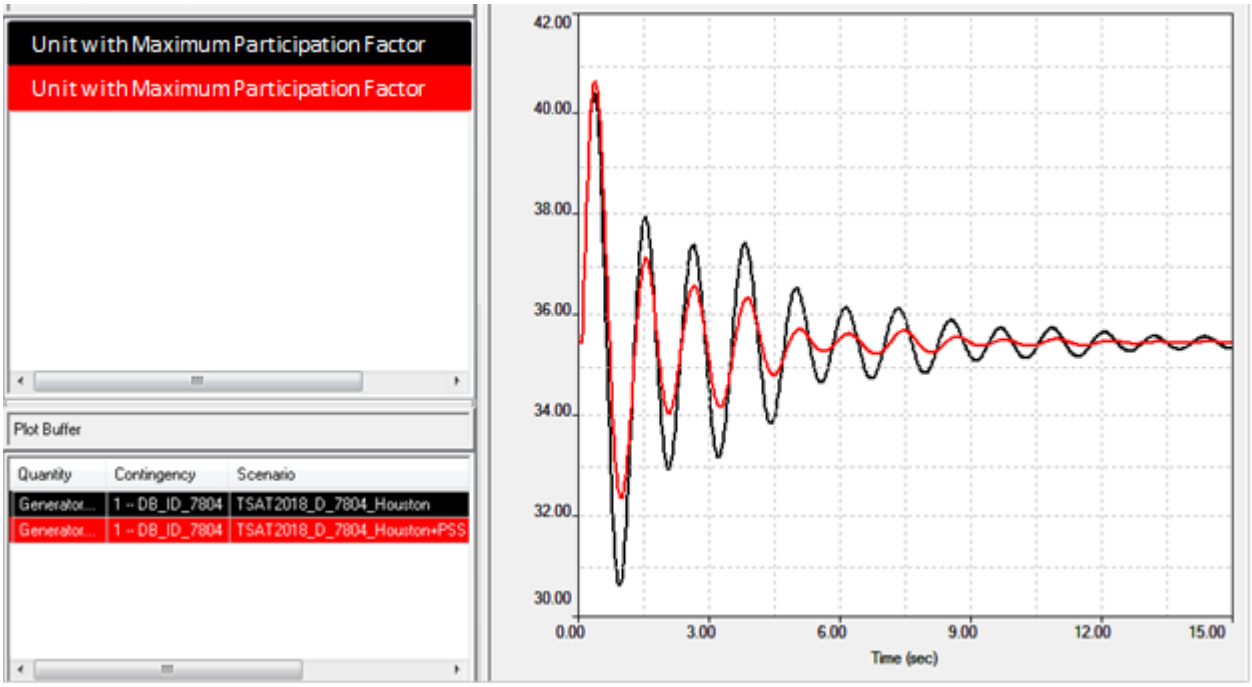

Figure 6-9: New PSS Performance for the Critical Inter-area Mode.

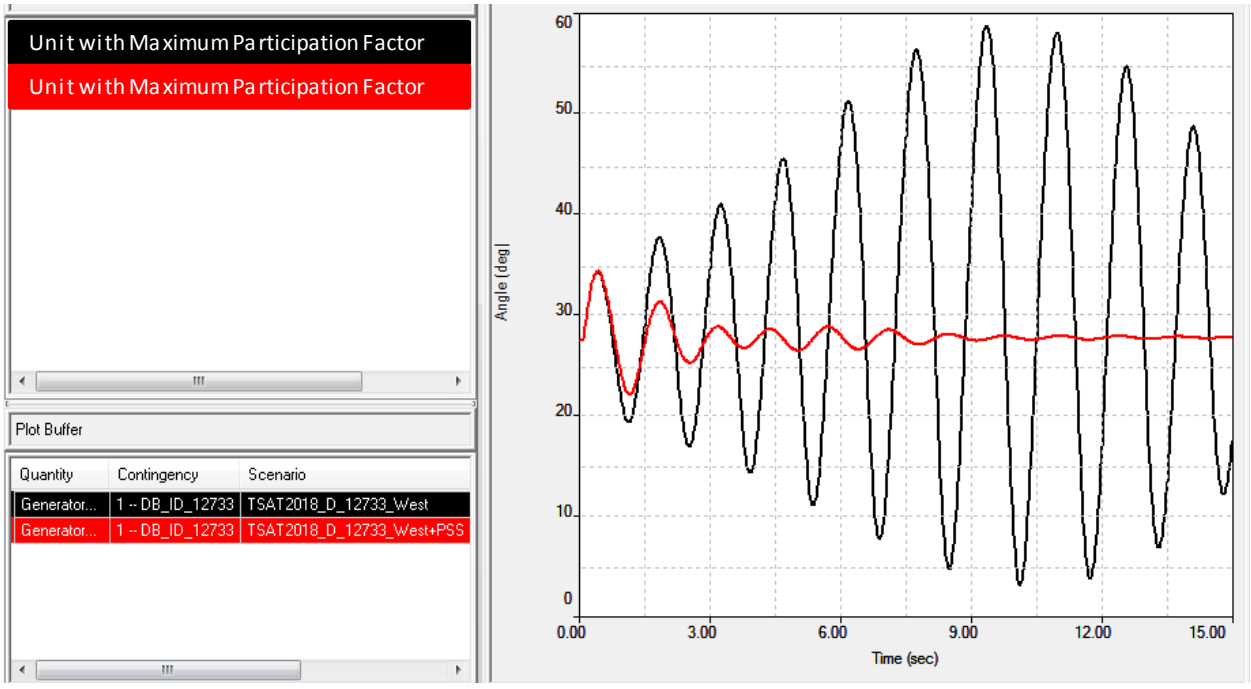

Figure 6-10: New PSS Performance for the Critical Local (Two-plant) Mode.

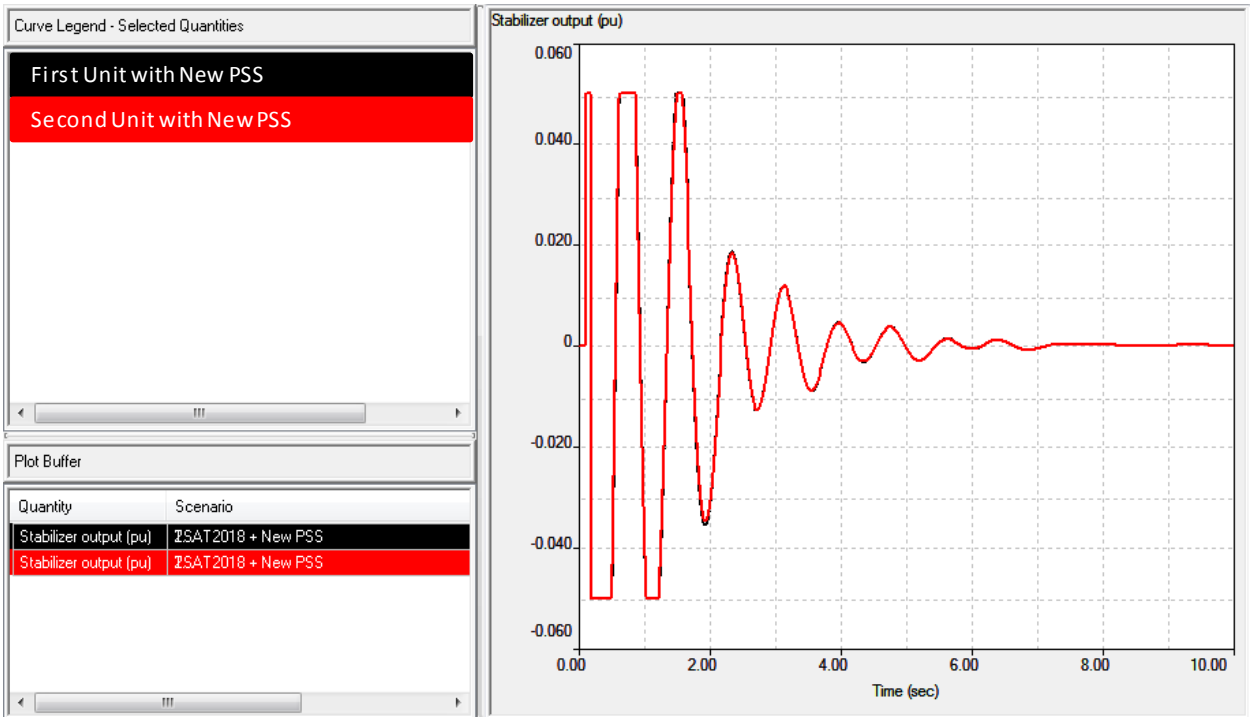

Figure 6-11: New PSS Output for the Large Disturbance #1.

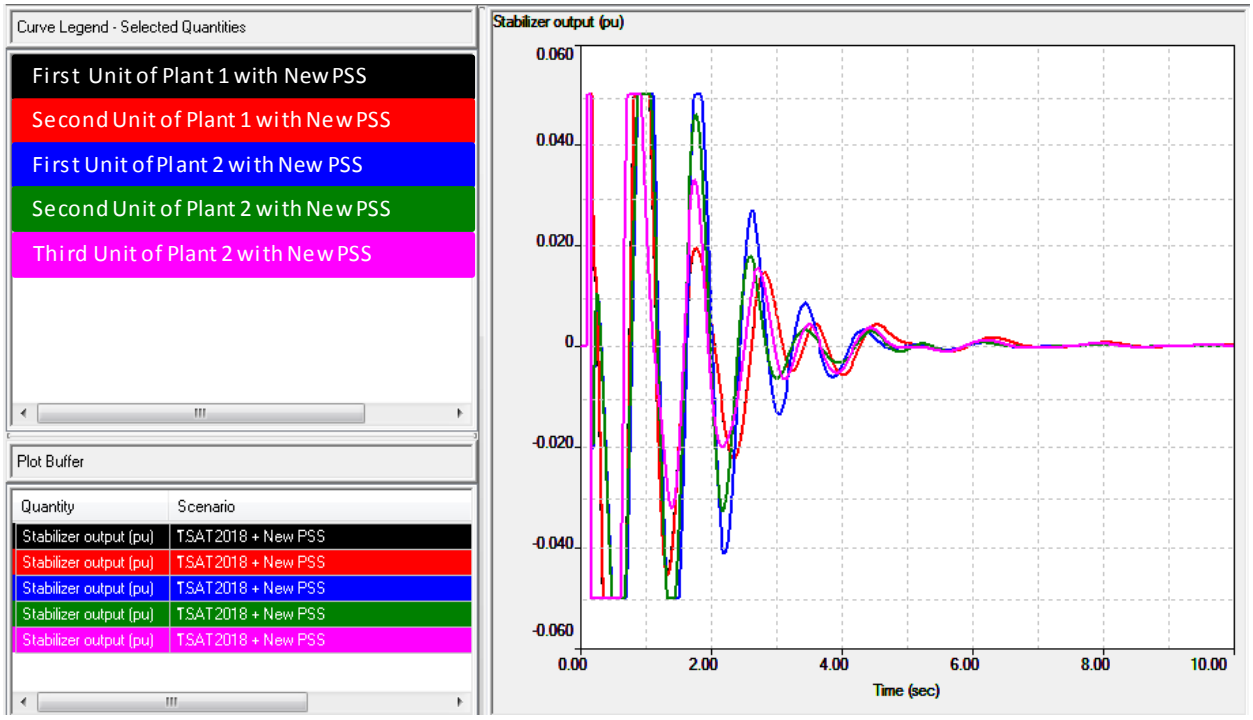

Figure 6-12: New PSS Outputs for the Large Disturbance #2.

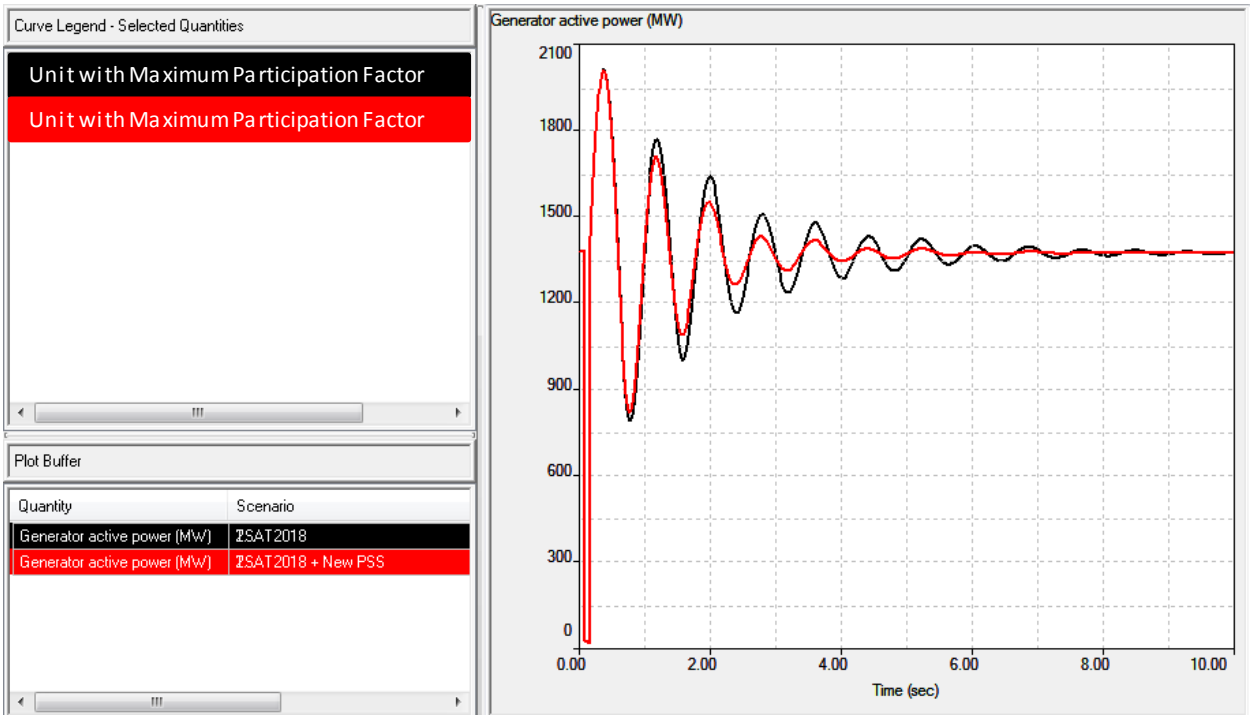

Figure 6-13: Active Power Comparison for the Large Disturbance #1.

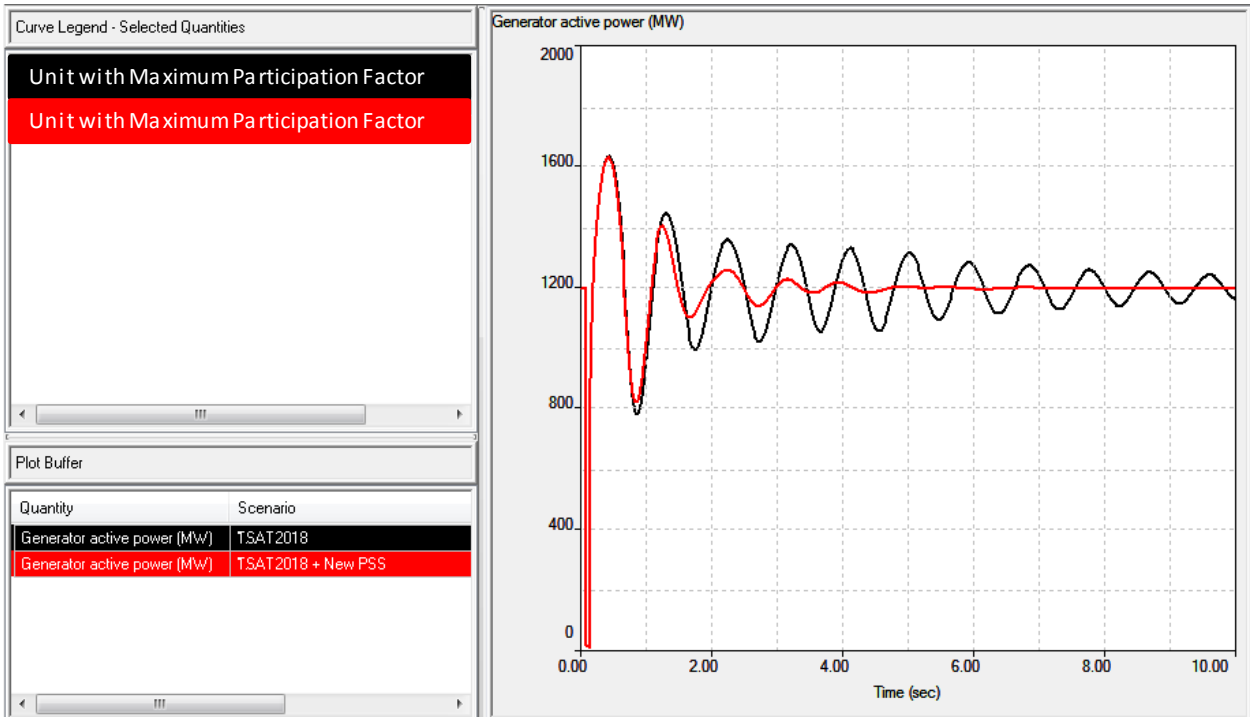

Figure 6-14: Active Power Comparison for the Large Disturbance #2.

6.5 Performance of the Existing PSS

The existing PSS performances before and after tuning were checked using both SSAT and TSAT. Eigenvalue and time-domain simulations were in close agreement and both indicated adequate damping. Note that the main purpose for tuning the existing PSS is not to increase damping, as there has been sufficient damping in all scenarios, with the exception of the two extreme situations that required new PSS. The emphasis has rather been on removing possible adverse effects on synchronizing torques, stability margins for control modes, torsional filter performances, etc.

The existing PSS that are proposed for tuning in the field are the combination of those listed in Table 6-1 through Table 6-3, i.e., 39 of them in total. As the exciter models in these tables suggest, the actual associated exciters all appear to be fast and appropriate, as far as the PSS are concerned. Moreover, exciter step responses of TSAT did not show any slowness associated with these exciters either. Note that the final PSS gains may be adjusted in the field, especially those that were highly under-compensated before tuning; there are some implicit gain increases associated with the increased phase compensations, as was demonstrated earlier in this section.

As the phase compensation results indicated, a number of over-compensated PSS needed correction, which might result in reduced (rather than increased) damping. Similar conclusion applies to those with reduced gain. As a result, while the overall damping changes are small (some higher and some lower), the minimum damping ratios reported in Table 5-1 and Table 5-2 are maintained. The cases were also subjected to the two large disturbances that were used to check the new PSS gains and limits for comparison of the existing PSS before and after the proposed 39 tuning sets. The outputs of all PSS for FY2018 and HWLL2016 base case simulations are presented in Figure 6-15 through Figure 6-22. These results indicate better performance after tuning, as in general the PSS perform their duties without prolonged saturated outputs, as well as with somewhat smaller activities afterwards.

The HWLL2016 plots suggest that the outputs of the IEEEST PSS at two units may remain saturated for several cycles; their gain reduction (say from 1.5 to 1.0) is a good idea, but not a critical issue.

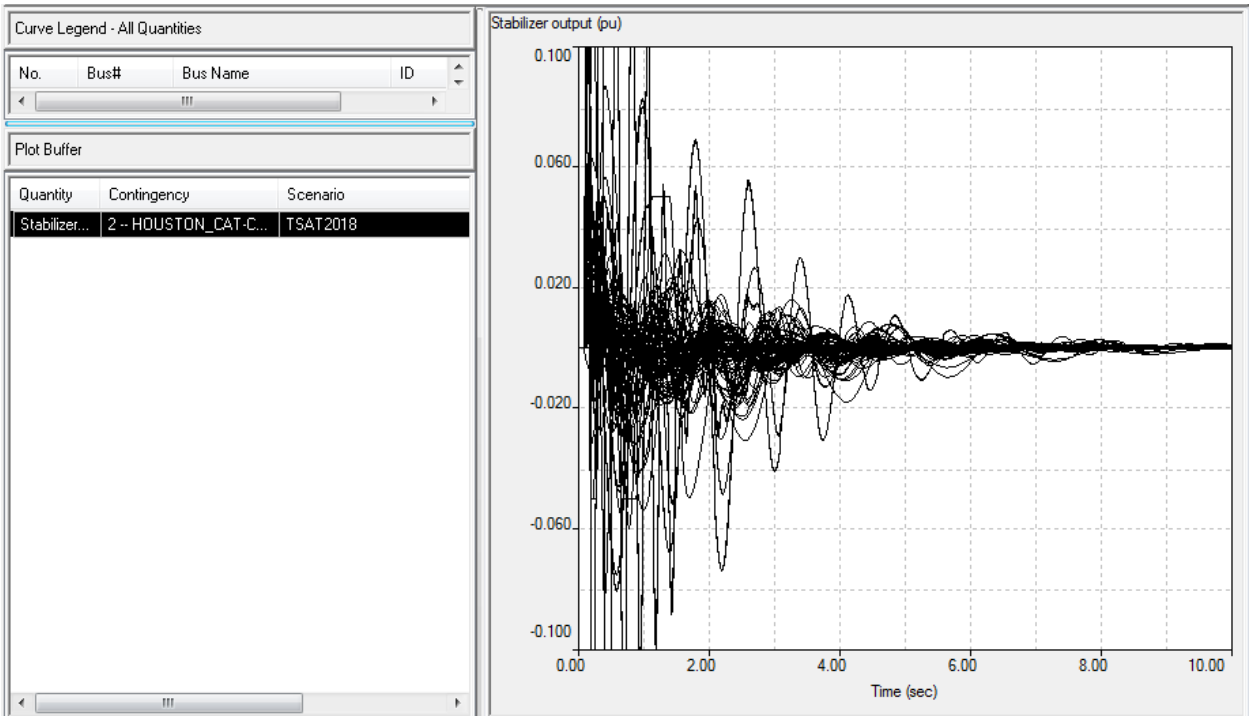

Figure 6-15: Existing PSS Outputs for the Large Disturbance #1 – FY2018 Base Case before Tuning.

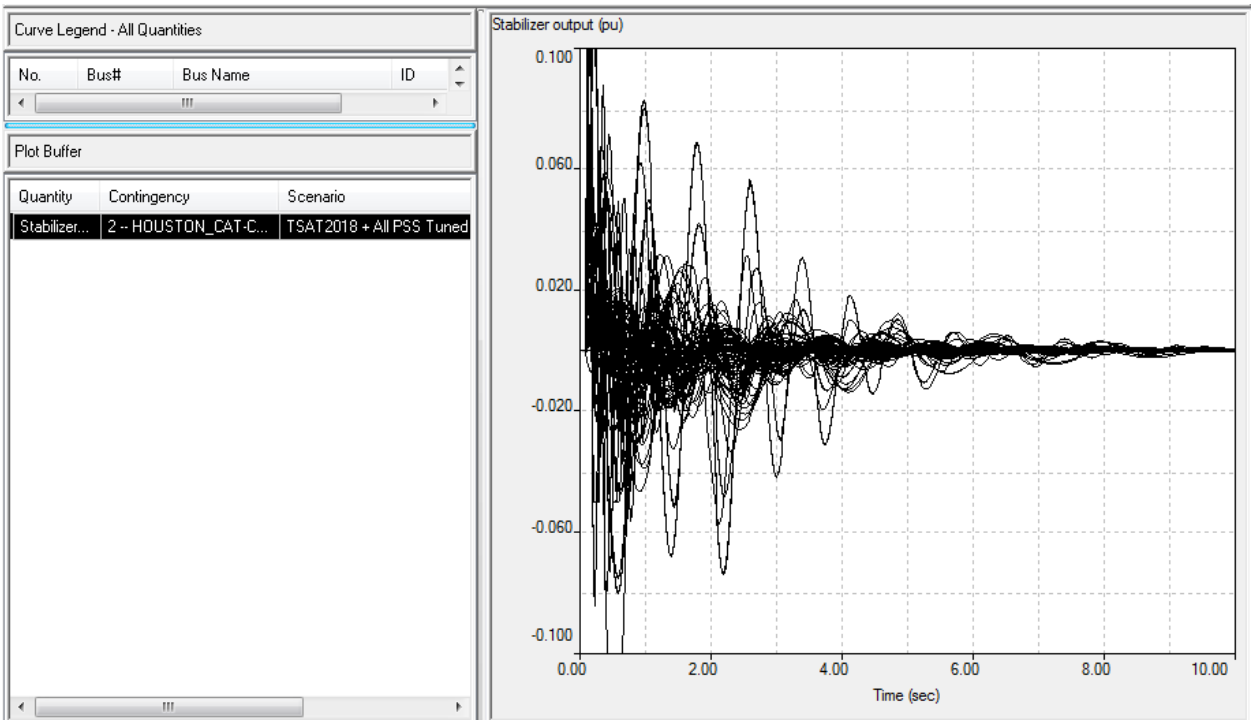

Figure 6-16: Existing PSS Outputs for the Large Disturbance #1 – FY2018 Base Case after Tuning.

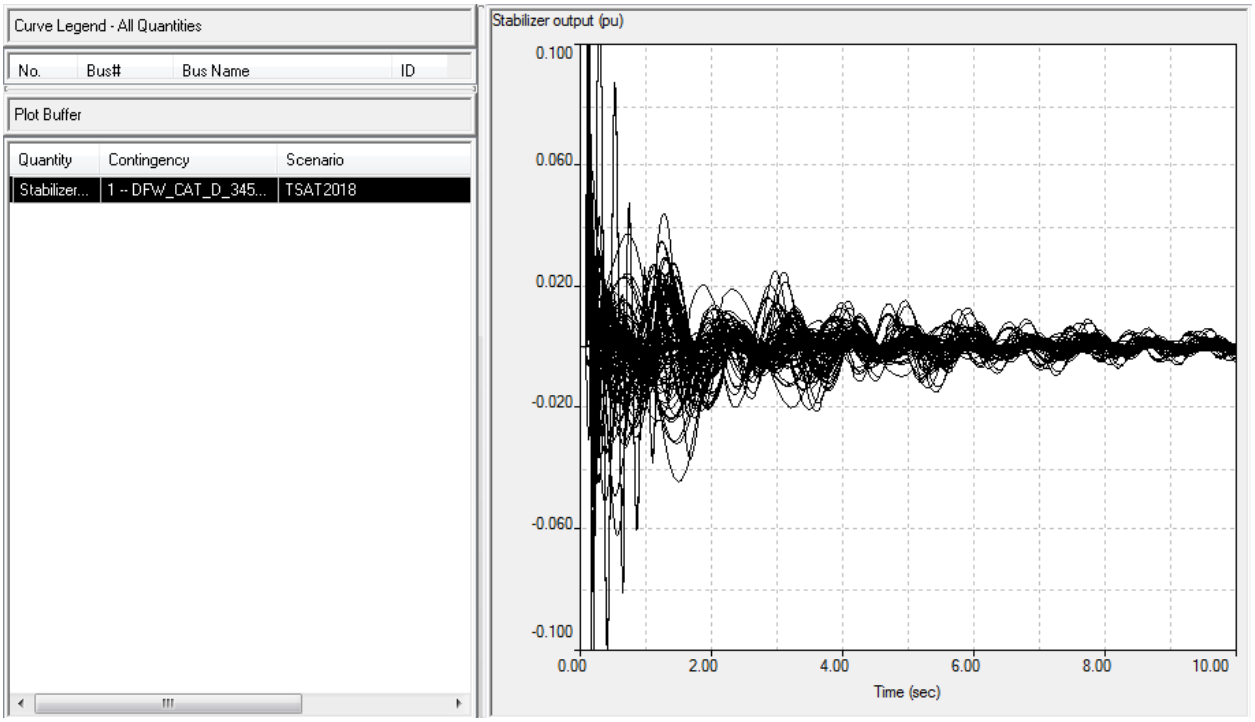

Figure 6-17: Existing PSS Outputs for the Large Disturbance #2 – FY2018 Base Case before Tuning.

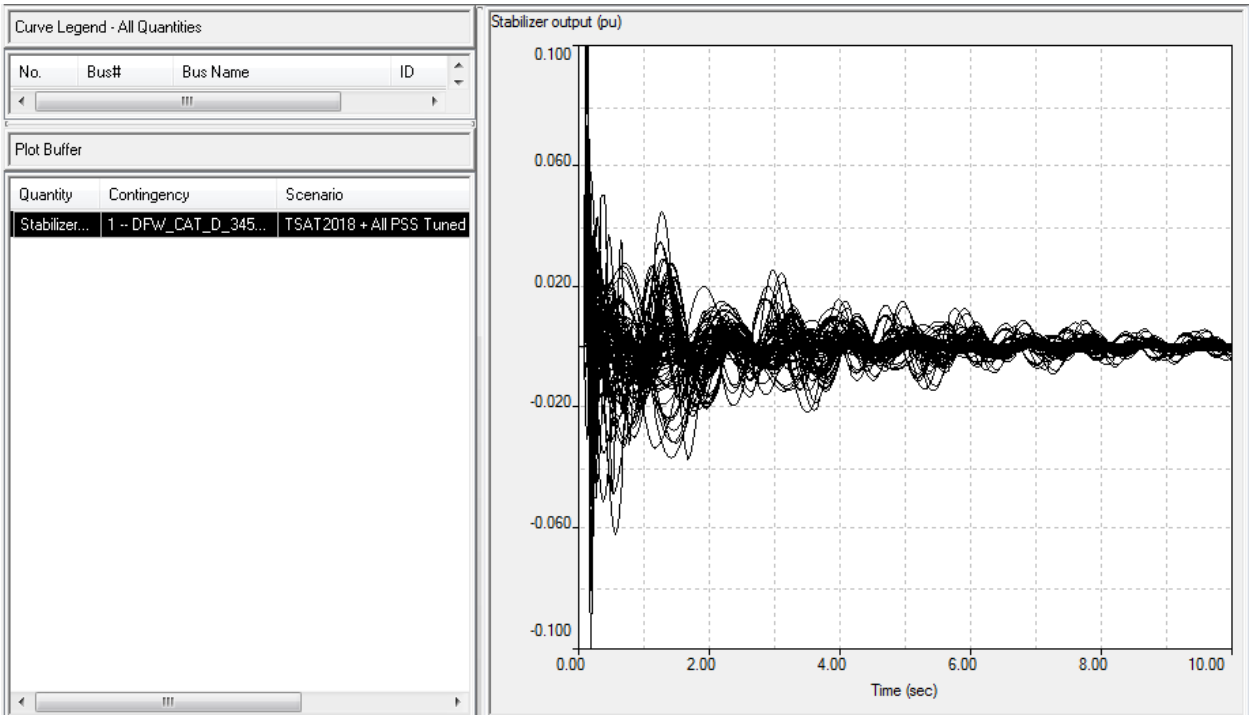

Figure 6-18: Existing PSS Outputs for the Large Disturbance #2 – FY2018 Base Case after Tuning.

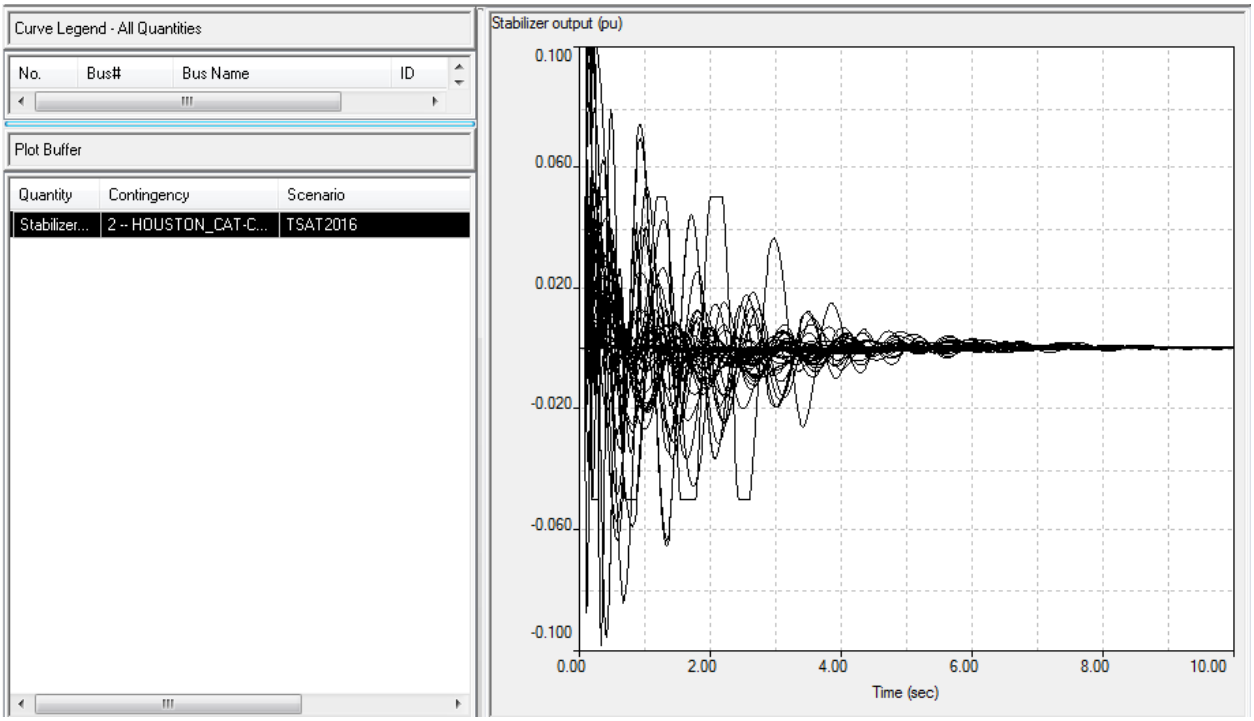

Figure 6-19: Existing PSS Outputs for the Large Disturbance #1 – HWLL2016 Base Case before Tuning.

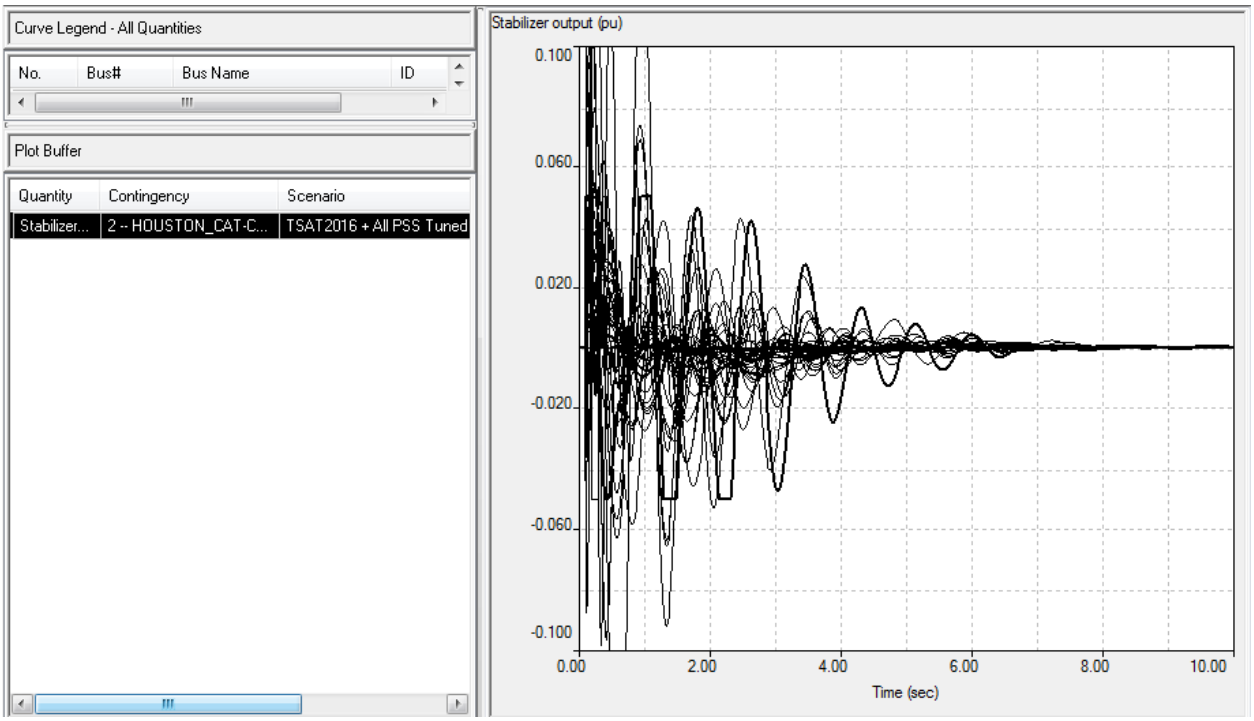

Figure 6-20: Existing PSS Outputs for the Large Disturbance #1 – HWLL2016 Base Case after Tuning.

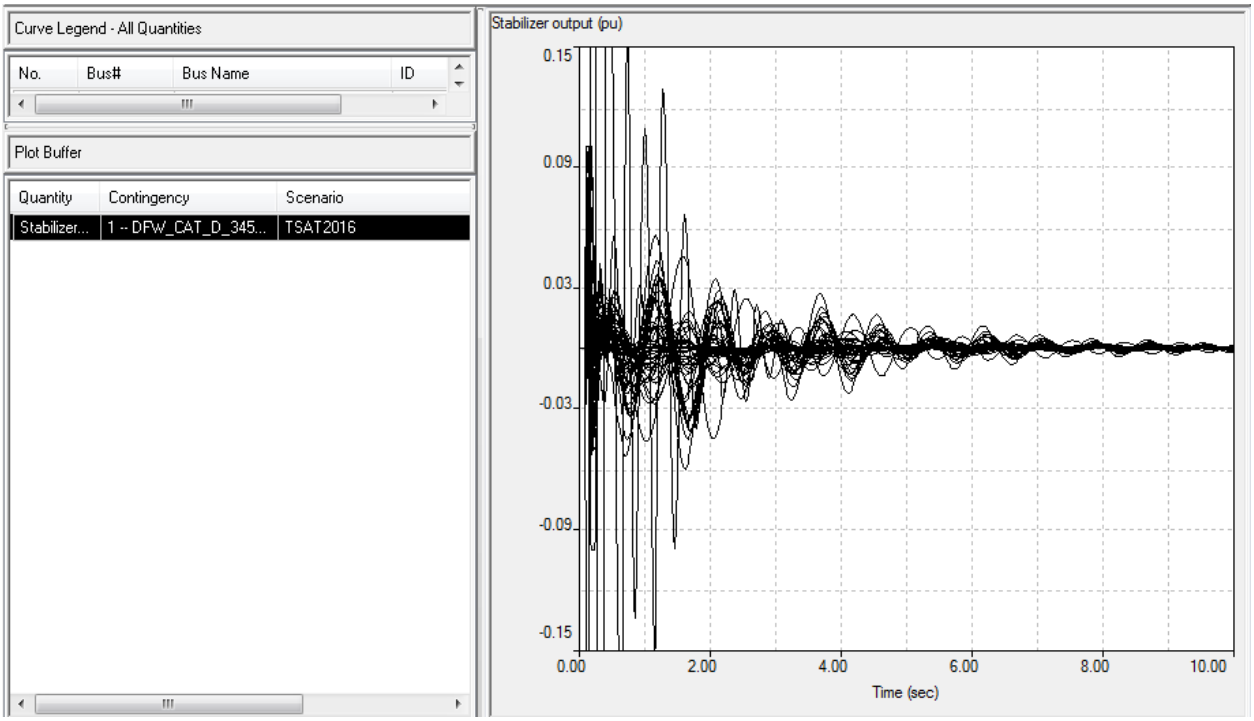

Figure 6-21: Existing PSS Outputs for the Large Disturbance #2 – HWLL2016 Base Case before Tuning.

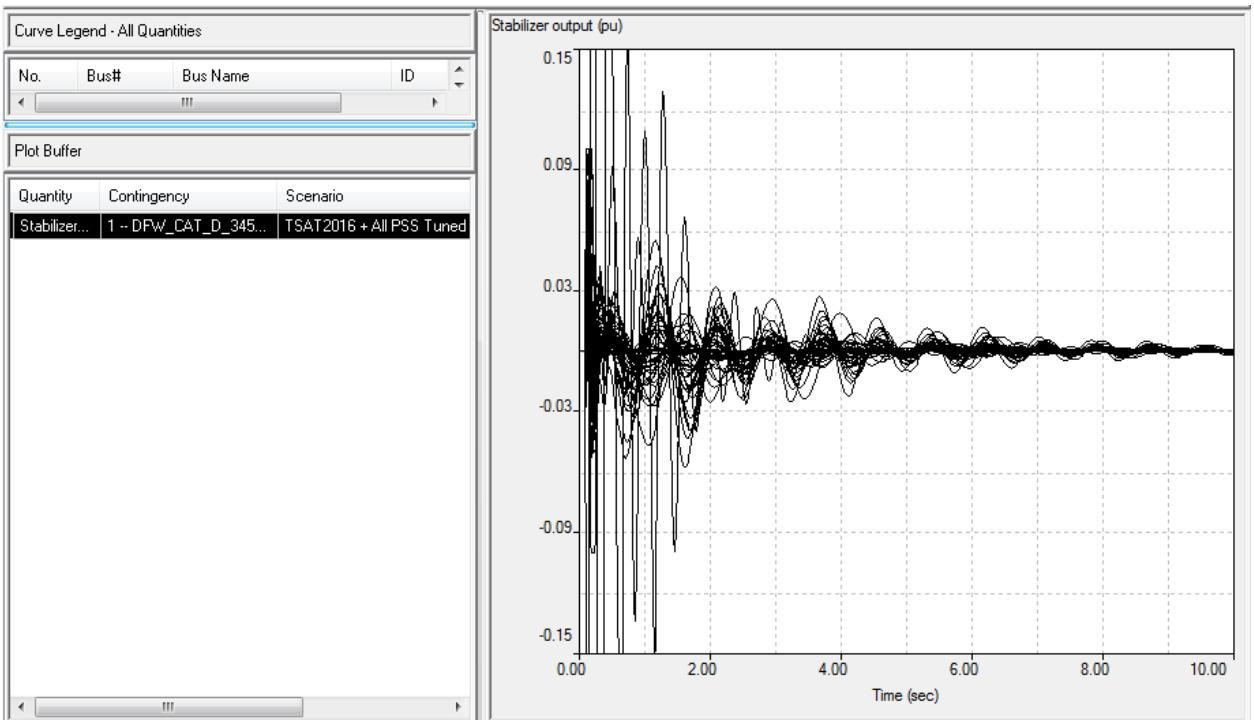

Figure 6-22: Existing PSS Outputs for the Large Disturbance #2 – HWLL2016 Base Case after Tuning.

6.6 Assessment of a Recent Event in Houston

Multiple oscillations were captured at multiple generators within the Houston region between July and September 2012, which are summarized as follows:

1) *11:41 PM, July 30, 2012.* The oscillation was sustained for about four minutes until all units of a certain plant (designated here as plant X) ramped down to zero MW output. There was no known transmission grid disturbance or switching and notable oscillations were observed only at units inside and around the Houston region, including STP units.
2) *10:30 PM, August 13, 2012.* The oscillation was sustained for two minutes and diminished after unit 3 of plant X was manually tripped due to large power (MW and MVAr) swing. There was no known transmission grid disturbance or switching. Units 1, 2, and 4 of plant X were ramped down to zero MW about five minutes after its unit 3 tripped. Notable oscillations were observed only at units inside and around the Houston region, including STP units.
3) *07:35 AM, September 27, 2012.* The oscillation was sustained for one minute and diminished after units 2, 3, and 4 of plant X tripped. Its unit 1 was slowly ramped down and went off line two minutes later after oscillation was diminished. Before the oscillation a 345 kV transmission line switching occurred.
4) *11:00 AM, September 27, 2012.* Testing was being performed to identify the cause of oscillations, which included disabling the AVR for unit 4 of plant X. The oscillation was sustained for about one minute and diminished after its unit 3 tripped. There was no known transmission grid disturbance or switching.

After the last incident dynamic simulations were performed by tuning unit 4 exciter of plant X to re-create the oscillatory mode. Although the results did not conclude that this unit was the cause of the oscillations, the choice of investigating a control issue related to this particular unit was consistent with the high magnitude of power oscillations observed at plant X in all of the above incidents. The oscillation frequency observed in the simulation results was in the range of 1.2~1.8 Hz, i.e., a typical frequency range for interplant oscillations.

In this project we did not observe such a mode in any of the studied scenarios, which also included performing single-plant-infinite-bus eigenvalue scans for all generating plants in Houston region. This is not surprising as the information about the incidents suggest that a specific control issue may have caused them, especially since they mostly occurred without any major contingency. In this context, we were able to re-produce simulation results similar to those mentioned above by simply inverting the sign of the K_F/T_F feedback loop in the EXST1 exciter model of unit 4.

Eigenvalue analysis of both FY2018 and HWLL2016 base cases with this control sign inversion revealed an oscillation around 1.3 Hz with a large negative damping, i.e., an unstable control mode related to one machine only (and not an interplant mode); SMIB simulation of unit 4 produced virtually the same mode. The shape of this mode points out very high, and almost exclusive, observability of the oscillation in Houston region. It also indicates that the oscillation should be generally observable at the unit causing this kind of problem more than at any other unit in the

system (although could be somewhat disturbance-dependent as well). Obviously, addition of more PSS to the system and/or tuning the existing PSS could not improve a control problem of this nature.

Time-domain simulations shed more light on the re-produced oscillation behavior. As can be seen from Figure 6-23, the active power oscillation magnitude reaches a limit, which depends on a number of system conditions including the initial loading of unit 4. The oscillation was triggered by tripping a 345 kV transmission line, although any nearby small disturbance would have produced similar results.

Prony analysis computed the frequency of oscillation in the range of 1.2~1.3 Hz in various simulations. The mode may appear to have almost zero damping, but this is due to the exciter limits (which were absent in the linearized model of eigenvalue analysis), preventing the responses from further growing, as demonstrated by the field voltage responses in Figure 6-24. The initial output of unit 4 is 132.3 MW in the original FY2018 case and 31.0 MW in its reduced (minimum) output scenario. The corresponding sustained peak-to-peak power oscillations are about 202 MW and 61 MW, respectively.

Problems of the above nature can be avoided by regularly performing validation field testing on generators and their controls.

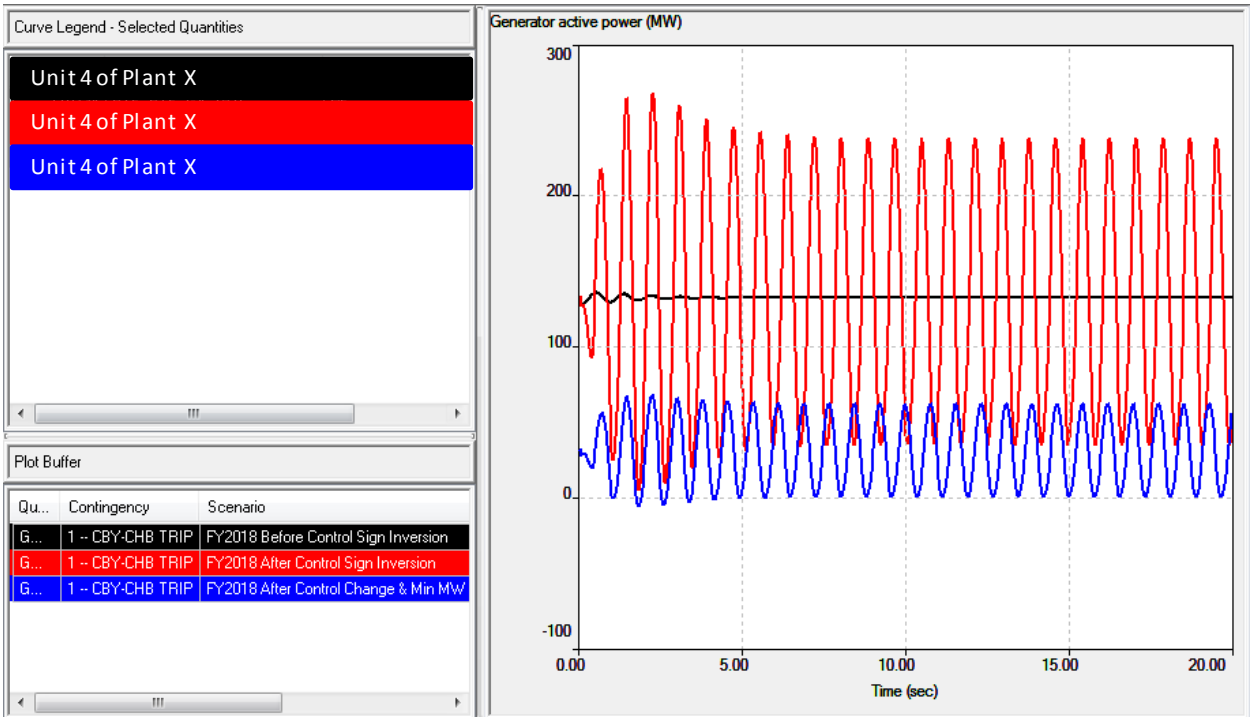

Figure 6-23: Active Power Responses of Unit 4 of Plant X before and after Sign Inversion in Its Exciter – FY2018 Base Case.

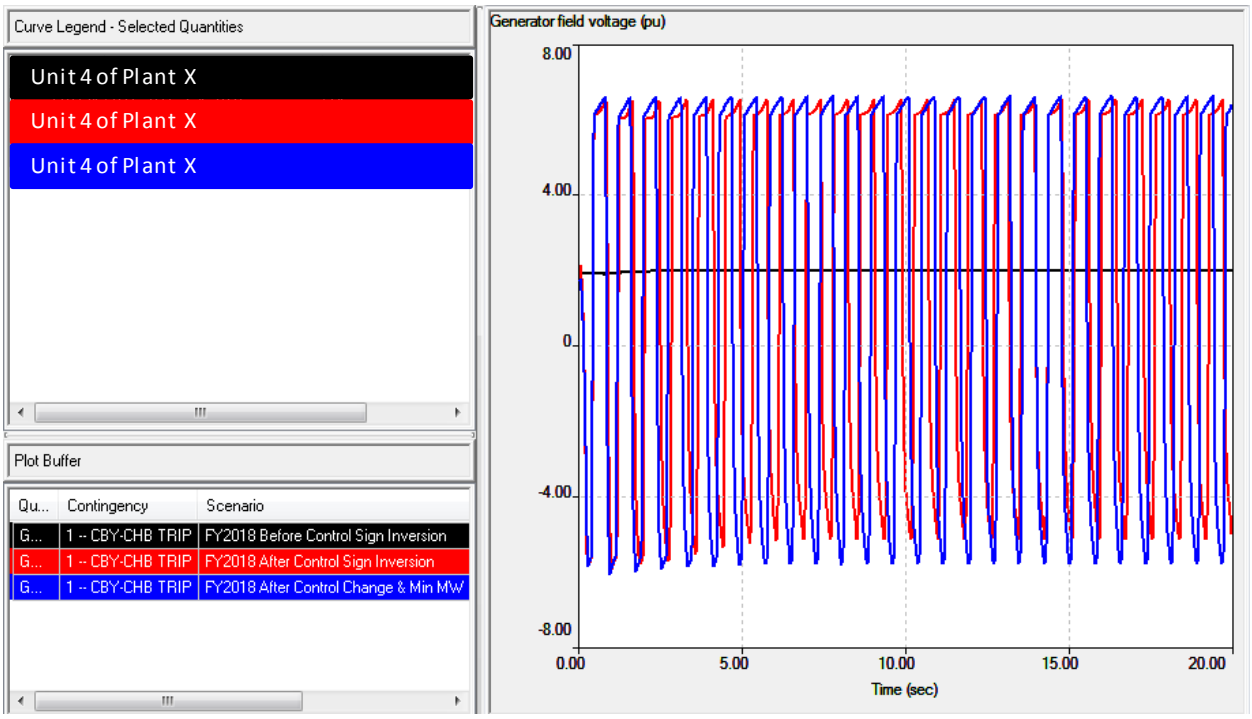

Figure 6-24: Field Voltage Responses of Unit 4 of Plant X before and after Sign Inversion in Its Exciter – FY2018 Base Case.

6.7 Comparison with the Previous Study of the Same Nature

A similar study of the ERCOT system was performed by Powertech in 2001-2002 [4]. Its main findings were reported to be two critical inter-area modes, one north-south and one east-west, especially for some stressed scenarios under the 2004 peak load conditions. Furthermore, while the worst contingencies occurred around the Houston – San Antonio – Corpus Christi triangle, the PSS in AEP_TCC (east) area appeared to be very effective in providing sufficient damping for these modes.

Relating the above to the findings of the present study is not a straightforward task. The changes in the system are very significant in terms of generation plants and their controls, loads, and transmission network. For example, between 2004 and 2018 conditions the peak load has increased from 66.9 GW to 79.7 GW, i.e., 19.1% increase, with similar increase in generation. Moreover, the number of in-service PSS has dramatically increased from 50 to 164. Significant topology improvements have also occurred, especially at the 345 kV level. As a result, the overall effects of these changes on system damping appear to be quite positive, which minimizes the chance for finding modes similar to those of the previous study.

While the same Houston – San Antonio – Corpus Christi triangle turned out to be still the most critical region in terms of contingencies and observing/controlling the critical inter-area oscillations, the AEP_TCC PSS did not play a critical role anymore; the latter was confirmed by removing the 18 PSS of FY2018 (or 8 PSS of HWLL2016) in AEP_TCC area without degrading effect on damping. Removal of all 164 PSS in the FY2018 base case, however, revealed an inter-area mode with poor damping (to be even worse after contingencies), which has a north-south shape close to that of the previous study; even the frequency of oscillation is close.

7. Conclusions

A comprehensive small-signal stability analysis has been performed for the ERCOT interconnected system. The study was focused on the following aspects:

- Examining the small-signal stability behavior of the ERCOT system;
- Proposing new Power System Stabilizers (PSS) in the ERCOT system to provide optimal damping for the identified critical modes;
- Tuning the existing PSS in the ERCOT system to provide optimal performance in the whole system without adverse effects;
- Identifying the best Phasor Measurement Unit (PMU) locations for oscillation monitoring;
- Reviewing/sanity checking of the ERCOT stability data.

The small-signal stability analysis was conducted for the following system representations:

- 2 loading conditions, i.e., peak load and light load with high wind generation;
- 5 transfer patterns for each loading condition;
- N-1, N-2, and N-x contingencies for all transfer patterns and loading conditions.

The voltage stability limits of the transfers were found for the considered contingency types and their corresponding power flows were created for the comprehensive small-signal stability analysis, along with the sanity checked and corrected matching dynamic data.

7.1 Summary of the Findings

The findings of the study are summarized below:

- All scenarios showed sufficient damping under N-0, N-1, and N-2 contingency situations.
- One local (two-plant) mode was identified that could have even negative damping under certain extreme contingency (N-x) conditions. Participation factors of the mode suggested addition of new PSS for 5 units of two plants, which were tuned and assessed using both eigenvalue analysis and time-domain simulations. The units of the first plant have higher effect than the units of the second plant, and are by themselves capable of fulfilling the typical 3% damping criterion. However, both sets are needed to reach beyond 5% damping, which is a more desirable criterion for local modes.
- One inter-area mode was identified that could have poor damping in certain extreme contingency (N-x) situations. Participation factors of the mode suggested addition of new PSS for units, which were tuned and assessed using both eigenvalue analysis and time-domain simulations. These PSS are not a must in terms of fulfilling the typical 3% damping ratio, but they provide the additional benefit of diminishing power oscillations of these units in a much

shorter time span and even reducing the first swing peak-to-peak oscillation. They also provide for higher damping margin against the uncertainties associated with load models, etc. The next best units are much less effective as their participation entries are drastically smaller.

- Adverse effects of the transfers and load dynamics on the damping situations were moderate.
- The light load scenarios consistently revealed better damping situations than their corresponding peak load scenarios. Despite fewer synchronous generators (and thus fewer PSS) in the light load case, the higher damping is consistent with generally milder flows through the network due to lower loading.
- The existing PSS were tuned to provide optimal damping without adverse effects on synchronizing torques, stability margins for control modes, torsional filter performances, etc. The tuning procedure was described in detail and the tuned parameters were provided. The tuned parameters were also verified under a wide range of system conditions and contingencies using both eigenvalue analysis and time-domain simulations. At the end, 39 PSS were recommended to be tuned in the field.
- The best PMU locations for oscillation monitoring were identified based on voltage magnitude mode shapes of the eigenvalues with the lowest damping ratios. As a result, 34 buses were ranked, from which ERCOT may choose, considering the suitability of the associated substations for PMU installation (or availability at present).
- The oscillations in the 2012 Houston event were most probably a control issue at some unit in the region and not an interplant mode that could be improved by PSS.
- Comparing to the 2001-2002 study of similar nature, while the same Houston – San Antonio – Corpus Christi triangle turned out to be still the most critical region, the PSS in AEP area did not play a critical role anymore. Furthermore, the increase in renewable generations did not impose a negative effect on damping.

The substations for installation of PMUs to monitor inter-area oscillations may be selected from the ranked list below. In particular, the first four substations provide high observability for all six modes, although inclusion of more locations may be considered to increase the reliability of the monitoring system. Once a location is chosen, however, any nearby bus is redundant and may be skipped.

#	Bus # [Name]	#	Bus # [Name]	#	Bus # [Name]
1	8905 [NEDIN7C 345.]	13	3105 [ELKTON_5345.]	25	45500 [T_H_W___345.]
2	5915 [SO_TEX__345.]	14	45971 [KUYDAL74345.]	26	46100 [N_BELT__345.]
3	3100 [MARTINLK345.]	15	3103 [SHAMBRGR345.]	27	40700 [GRNBYU__345.]
4	40600 [ROANS___345.]	16	3119 [NACOGDSE345.]	28	3130 [FOREGROV345.]
5	44645 [SNGLTN_3345.]	17	46290 [RTHWOD__345.]	29	3124 [TRINDAD2345.]
6	967 [GIBN_CRE345.]	18	3117 [LUFKNSS_345.]	30	3123 [TRINDAD1345.]
7	45972 [KUYDAL75345.]	19	80307 [DELSOL7B345.	31	80355 [DELSOL7A345.
8	42500 [DOW_____345.]	20	8902 [RIOHONDO345.]	32	43035 [OASIS___345.]
9	46500 [TOMBAL__345.]	21	44900 [ZENITH__345.]	33	5966 [LALTA345345.
10	3102 [TYLERGND345.]	22	8164 [COLETO7A345.]	34	43030 [MEADOW__345.]
11	3116 [MTENTRPR345.]	23	44200 [HILLJE__345.]		
12	3109 [STRYKER_345.]	24	40900 [KING____345.]		

7.2 Recommendations for Future Studies

The study reveals that small-signal stability is indeed a security concern for the ERCOT system and PSS plays an essential role in providing sufficient damping to the major oscillatory modes. It is therefore recommended that similar studies be performed regularly to ensure the small-signal security of the system. The following may serve as guiding indicators for initiating future studies of this nature, especially if they occur in the areas that are already identified to be prone to damping issues:

- Addition/retirement of sizable generation (and generator controls);
- Significant load increases, both static (non-rotating) and dynamic (induction motors);
- Major expansions/interconnections of the transmission system;
- Indication of a poorly-damped oscillation in the system by monitoring devices.

Furthermore, the following may be emphasized in future studies of similar nature:

- Completeness of the dynamic data as much as possible (including load models);
- Accuracy of the data, particularly for the generator excitation system models (including PSS), which can be achieved by performing field testing on generators and validating/deriving appropriate models using the corresponding measurements;
- Study scenarios being representative of the actual, and yet critical, system conditions, so that the worst damping situations can be captured and prevented from becoming security concerns.

8. References

[1] EPRI Report TR-108256, "System disturbance stability studies for Western System Coordination Council (WSCC)", Prepared by Powertech Labs Inc., September 1997.

[2] P. Kundur, *Power System Stability and Control*, McGraw-Hill, 1994.

[3] CIGRE Task Force 38.01.07, "Analysis and Control of Power System Oscillations," CIGRE Technical Brochure, December 1996.

[4] Report 13131-21-00-001, "Small Signal Stability Analysis And Power System Stabilizer Tuning For ERCOT", Prepared by Powertech Labs Inc. for ERCOT, January 2002.

[5] Graham Rogers, *Power System Oscillations*, Kluwer Academic Publishers, 2000.

9. Appendix A: Weather and Service Areas and Zones of ERCOT

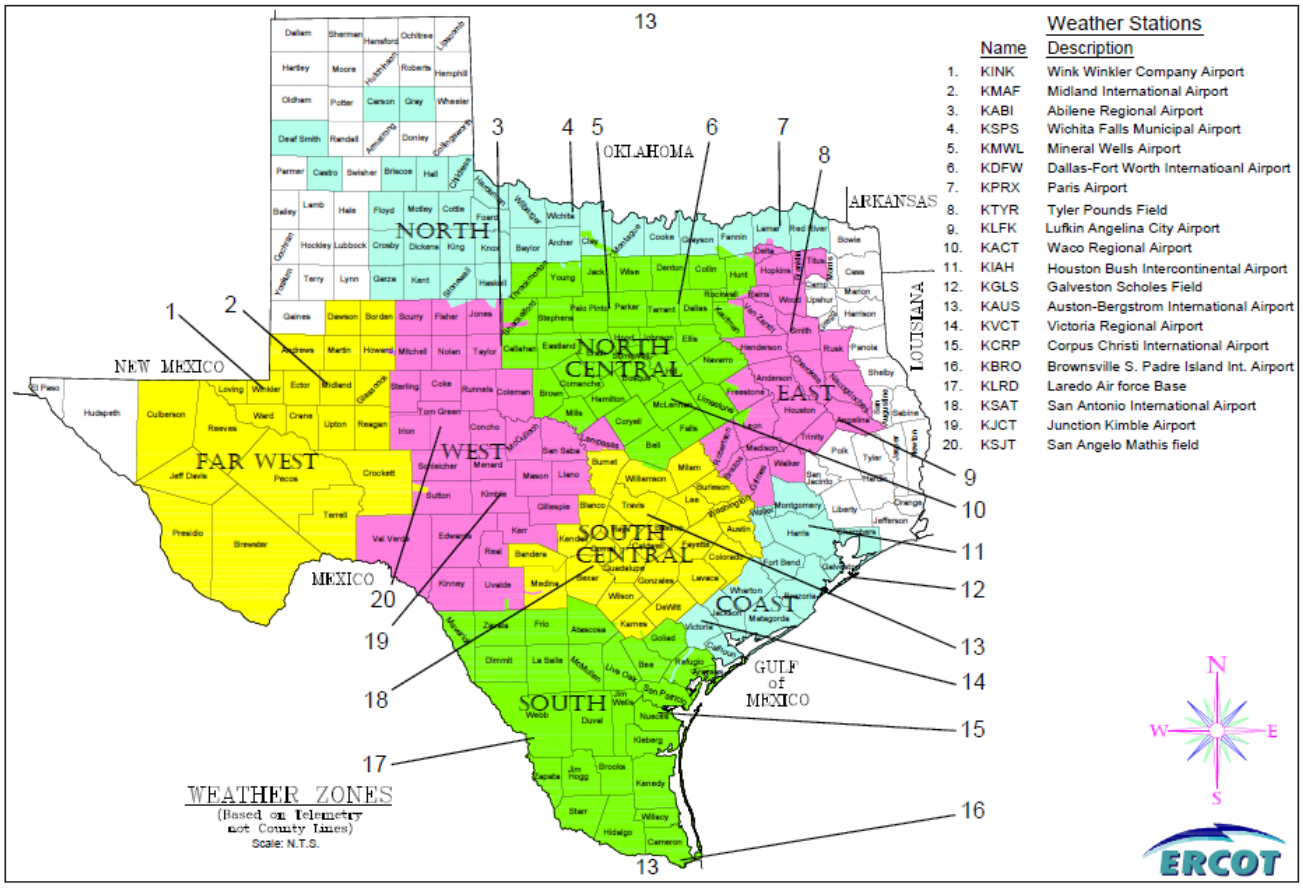

Figure 9-1: Weather Zones and Texas Counties.

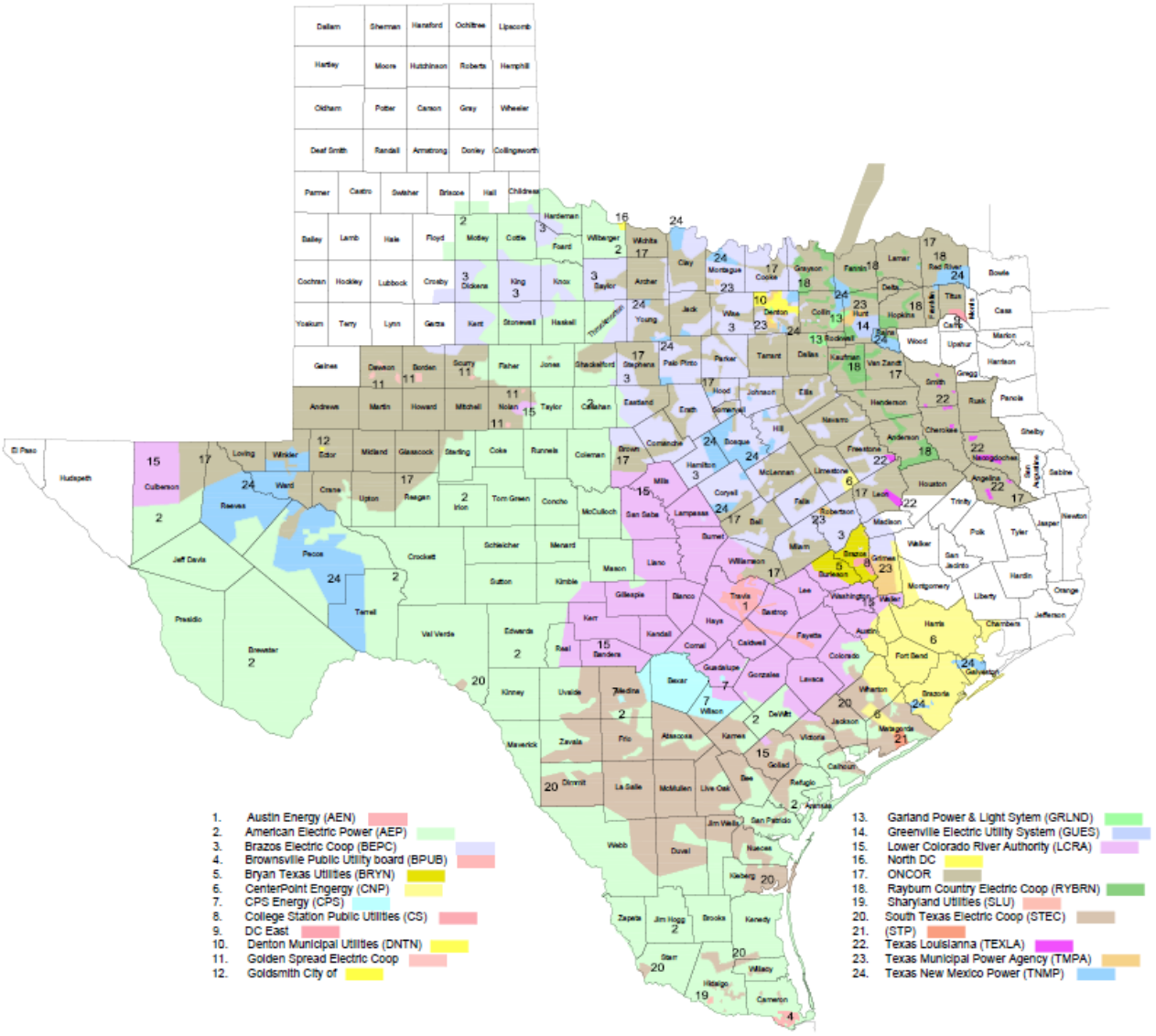

Figure 9-2: Service Areas/Zones of ERCOT.

10. Appendix B: Contents of the Transferred Files

… Final Report (Public).doc	This report (Word format)
… Final Report (Public).PDF	This report (PDF format)

10.1 VSAT Files

VSAT_2018_B.zip	Peak load VSAT cases with provided type B contingencies
VSAT_2018_B345.zip	Peak load VSAT cases with scanned type B contingencies
VSAT_2018_C.zip	Peak load VSAT cases with provided type C contingencies
VSAT_2018_D.zip	Peak load VSAT cases with provided type D contingencies
VSAT_2016_Bmin.zip	Interim VSAT Cases for running VSAT 2016 type B cases
VSAT_2016_B.zip	Light load VSAT cases with provided type B contingencies
VSAT_2016_B345.zip	Light load VSAT cases with scanned type B contingencies
VSAT_2016_C.zip	Light load VSAT cases with provided type C contingencies
VSAT_2016_D.zip	Light load VSAT cases with provided type D contingencies

10.2 SSAT Files

SSAT_FY2018.zip	Peak load SSAT cases for eigenvalue analysis
SSAT_FY2018_PMU.zip	Peak load SSAT cases for PMU placement
SSAT_FY2018_PSS.zip	Peak load SSAT cases for PSS verifications
SSAT_HWLL2016.zip	Light load SSAT cases for eigenvalue analysis
SSAT_HWLL2016_PMU.zip	Light load SSAT cases for PMU placements
SSAT_HWLL2016_PSS.zip	Light load SSAT cases for PSS verifications

10.3 TSAT Files

TSAT_2018_Killeen.zip	Peak load TSAT case with testing contingency
TSAT_2018_LowDamp.zip	Peak load TSAT cases for low damping verifications
TSAT_2018_PSS.zip	Peak load TSAT cases for PSS verifications
TSAT_2016_Killeen.zip	Light load TSAT case with testing contingency
TSAT_2016_LowDamp.zip	Light load TSAT cases for low damping verifications
TSAT_2016_PSS.zip	Light load TSAT cases for PSS verifications